Research Square

Preprints are preliminary reports that have not undergone peer review.
They should not be considered conclusive, used to inform clinical practice,
or referenced by the media as validated information.

Diversity and biolithostratigraphy of foraminifera from the Upper Eocene–Lower Oligocene Malishka section, Armenia

Taron Grigoryan
Institute of Geological Sciences
Lilit Sahakyan
lilitsahakyan@yahoo.com
National Academy of Sciences https://orcid.org/0000-0002-5539-5690
Elena Zakrevskaya
MUSEUM
Pavel Fokin
Moscow State University: Moskovskij gosudarstvennyj universitet imeni M V Lomonosova
Ara Avagyan
Institute of Geological Sciences

Research Article

Keywords: Stratigraphy, Lithofacies, Eocene-Oligocene Boundary, Microfossils, Nummulites

Posted Date: April 10th, 2025

DOI: https://doi.org/10.21203/rs.3.rs-6127696/v1

License: This work is licensed under a Creative Commons Attribution 4.0 International License.
Read Full License

Version of Record: A version of this preprint was published at Palaeobiodiversity and Palaeoenvironments on January 29th, 2026. See the published version at https://doi.org/10.1007/s12549-025-00692-z.

Diversity and biolithostratigraphy of foraminifera from the Upper Eocene–Lower Oligocene Malishka section, Armenia

Taron Grigoryan[1], Lilit Sahakyan[1,*], Elena Zakrevskaya[2], Pavel Fokin[3], Ara Avagyan[1]

[1]Institute of Geological Sciences, National Academy of Sciences of the Republic of Armenia, 24A Baghramyan ave., 0019 Yerevan, Armenia

[2] Vernadsky State Geological Museum RAS, Mokhovaya 11, bl.11 Moscow 125009, Russia

[3]Geological Faculty, Moscow State University, Vorobyevy Gory, 119991 Moscow, Russia

*Corresponding author e-maill: lilitsahakyan@yahoo.com

Abstract

The Eocene-Oligocene transition marks significant global climatic changes, coinciding with the closure of the southern Neotethys. The Priabonian-Rupelian transition in the Malishka section of the Vayots-Dzor area is represented by alternation of shallow-water limestones-sandstones with hemipelagic claystones and siltstones. These facies provide essential evidence for revising planktonic and benthic foraminiferal biozonations and analyzing the sedimentological characteristics of the section. In Malishka section turbidity currents are inferred from flute cast structures, reverse-graded bedding, and pebble-bearing limestone in the Late Eocene, which was followed by greywacke sedimentation in the Early Oligocene. Larger benthic foraminifers (LBF), fragments of solitary and colonial corals, red algae, echinoderms, bryozoans, bivalves and rare carbonate sponges, together with planktonic foraminifera (PF) in limestones suggest transport from the euphotic zone. The LBF exhibit significant abundance and diversity in the upper Eocene sediments, with about 20 species and subspecies of orthophragminids (*Discocyclina*, *Orbitoclypeus*, *Asterocyclina*) and nummulitids (*Nummulites*, *Operculina*, *Heterostegina, Spiroclypeus*). The Oligocene LBF are represented by only five species of *Nummulites*. The last occurrences of orthophragminids were observed before the Eocene/Oligocene boundary, as defined by PF zonation. About 40 species of PF are identified in the claystones and siltstones of uppermost Eocene and lower Oligocene. The 46-meter-thick Malishka section, spanning the Eocene/Oligocene boundary, corresponds to the PF zones E16, O1, O2 and O3 as well as the LBF zones SBZ20 and SBZ21. The study of PF and LBF from the Malishka section facilitated the correlation of bioevents between these two groups.

Keywords: Stratigraphy, Lithofacies, Eocene-Oligocene Boundary, Microfossils, Nummulites

1. Introduction

The Eocene–Oligocene transition (EOT) (35–33Ma) corresponds to a fundamental worldwide climatic and biotic reorganization (e.g. Krasheninnikov et al., 1986; Lear et al., 2000; BouDagher-Fadel, 2018), lasting about 500.000 years (Coxall & Pearson, 2007). It has been

detected on the early oxygen isotope records ($\delta^{18}O$) from deep-sea benthic foraminifera, latter recognised as a combination of continental ice growth and cooling (Lear et al., 2008). During this interval, global climate changes are characterized by three isotopic shifts: EOT-1, EOT-2 (Eocene-Oligocene transition) and Oi (Oligocene Isotope Event)-1 (Houben et al., 2012). EOT-1 is placed below the Eocene/Oligocene boundary (EOB), while EOT-2 and Oi-1 are placed above the EOB. The EOB is defined by the extinction of the spiny hantkeninid and smooth turborotalid planktonic foraminifera (PF) at 33.9 Ma (Vandenberghe et al., 2012; Wade et al., 2011; Hutchinson et al., 2021; BouDagher-Fadel, 2015). The secondary marker of this boundary is the highest occurrence (HO) of *T. cerroazulensis* group (Wade et al., 2018). The lowest occurrence (LO) of *Dentoglobigerina tapuriensis*, present in the Rupelian GSSP (Vandenberghe et al., 2012) is considered a zonal marker of the last century (Blow, 1979; Krasheninnikov et al., 1985). Orthophragminids and granulate *Nummulites* with a discoidal morphology disappeared close to the EOB (Less & Özcan, 2012). The correlation between events in PF and LBF at the base of the Oligocene remains unclear, with only a few investigations dedicated to this question (Cotton & Pearson, 2011).

Successions of siliciclastic deposits with intercalated carbonate layers are well preserved in several sections in Armenia, providing an opportunity to reconstruct the Eocene-Oligocene depositional history through integrated biostratigraphic analysis. For instance, the Landjar section in the Vedi area has been regarded as the type section for the base of the Oligocene in the former USSR (Krasheninnikov & Akhmet'ev, 1998). The Nummulitic and Mollusca zonations, firstly elaborated for the Eocene–Oligocene transition (e.g., Gabrielian, 1964; Grigorian, 1979; 1986) were added and described in terms of planktonic foraminiferal and nannofossil (Krasheninnikov et al., 1985), small benthic foraminiferal (Sahakyan-Gezalyan et al., 1967; Hayrapetyan, 2001, 2009) and palinomorph (Zaporozhets, 1989) zonations. Although significant progress has been made in recent decades in defining the modern biozonations based on LBF, PF, small benthic foraminifera (SBF), palinomorphs and radiolarians for the middle-upper Eocene strata (Cotton et al., 2017; Shcherbinina et al., 2017; Zakrevskaya et al., 2017, 2020; Sarkisova et al., 2020), the biozonation, as well as paleoenvironmental and paleogeographic conditions of the Eocene–Oligocene transition in low latitude settings of the Peri-Tethys and Northern Tethys areas remains poorly constrained.

The middle–upper Eocene part of a section near Malishka is well known from Gabrielian (1964), where the results of studies of nummulitids, orthophragminids, pelecypods and gastropods are summarized. Although this section is considered as a representative for the Hayots-Dzor Synclinorium, the Oligocene strata have not been thoroughly studied. For this section, Grigorian (1986) noted the presence of Oligocene *Nummulites,* while Krasheninnikov and Ptukhian (Krasheninnikov et al., 1985) briefly described the PF and *Nummulites* assemblages from the Priabonian and Rupelian parts of the section, highlighting the low diversity of foraminifera. The continuous succession of Eocene–Oligocene sediments with benthic and planktonic foraminifera in the Malishka Section offers the opportunity to define and apply regional zonation based on PF and LBF, as well as to correlate them with globarl biozones.

The aims of this study is to: 1) describe the sedimentological features of the section and perform paleoenvironmental reconstruction, 2) study the LBF and PF biostratigraphy based on their state-of-art taxonomy and biostratigraphic significance, and 3) detect additional zonal taxa of PF for uppermost Eocene – lower Oligocene.

2. Geological setting

The territory of Armenia is situated between remnants of two megacontinents: Gondwana to the south and Laurasia to the north. The South Armenian Block (SAB) is considered to have detached from Gondwana during the Late Triassic ~234 Ma (Nikogosian et al., 2023). The Alpine orogeny, driven by the convergence of Eurasian and SAB plates, led to the closure of the northern Neotethyan Ocean, shaping the region's geological evolution. The Armenian Highland includes the following orogenic terranes from south to north: the central part of the Taurids-Anatolides-South Armenian-Bitlis-Pütürge Microcontinent, the ophiolite nappe/suture zone, and the Eurasian margin (e.g., Sosson et al., 2010). The southern basement consists of Neoproterozoic metamorphic complexes overlain by pan-African Paleozoic predominantly sedimentary strata. According to many authors (e.g., Galoyan, 2008; Sosson et al., 2010), the Middle, Upper Jurassic ophiolitic complex outcrops in the Amasia-Sevan-Hagari suture zone (ASHSZ, Fig. 1A). This complex was emplaced southwards onto the South Armenian block (SAB) during the Late Cretaceous. Collision between the SAB and Eurasia started in the Late

Cretaceous, with uplift, further erosion and development of a Paleocene flexural basin in the frontal part of the suture zone (Sosson et al., 2010).

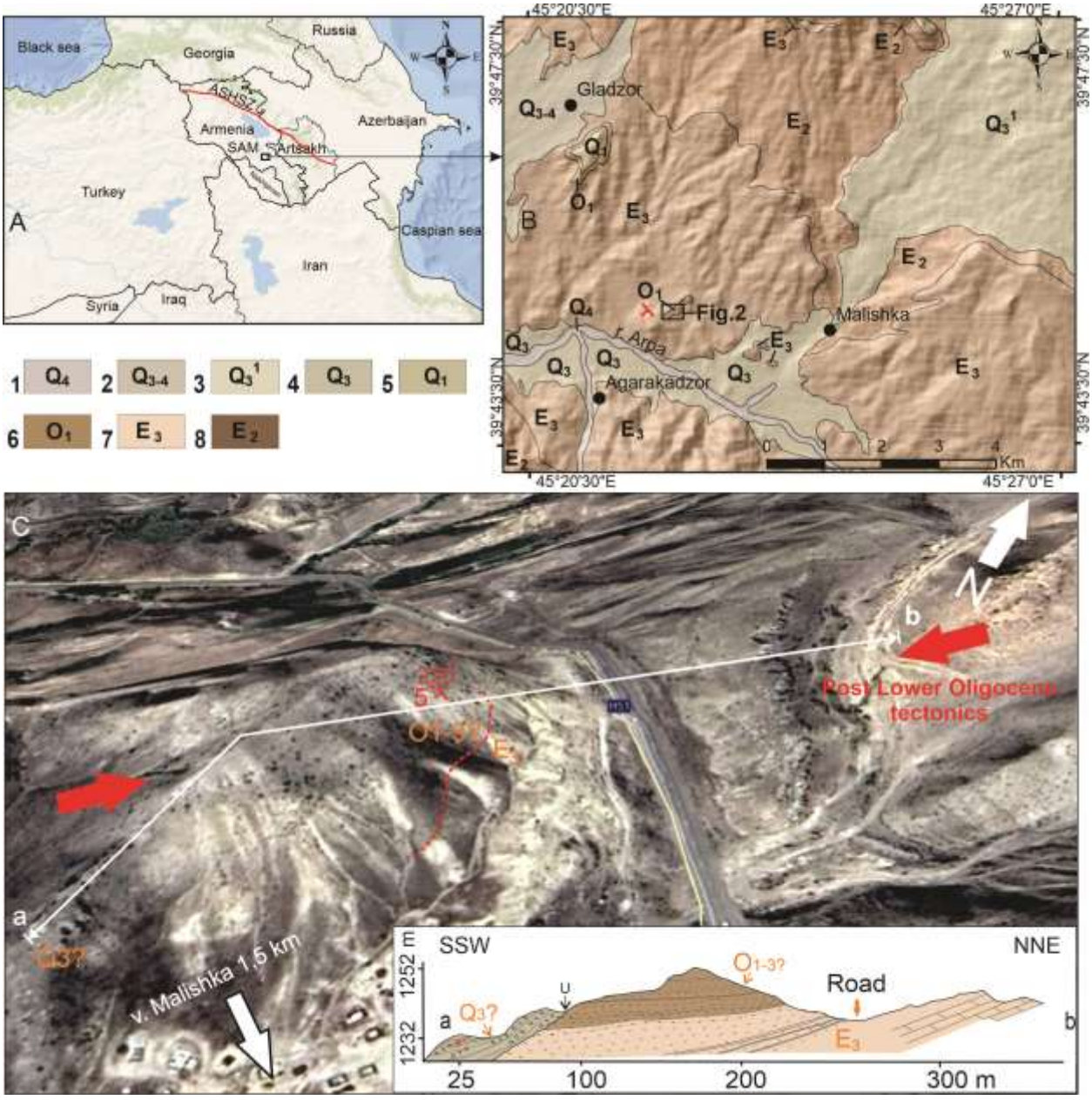


Fig. 1 A - Regional map showing the location of Armenia. ASHSZ-Amasia-Sevan-Hagari Suture Zone. B - The simplified geological map with Malishka section, modified after Markosyan et al. (1981). 1 Upper Quaternary sediments: alluvial sands, pebbles, sandy loams, 2 Upper Quaternary sediments, proluvial-deluvial crushed stone, 3 Upper Quaternary lavas, andesites, andesite-basalts, 4 Upper Quaternary sediments, boulders, gravels, sandy loams, 5 Lower Quaternary sediments, boulders, pebbles, conglomerates, travertines, 6 Lower Oligocene. Clays, sandstones, volcaniclastic breccias, volcaniclastic sandstones, 7 Upper Eocene. Limestones, sandstones,

112 calcareous clay, volcaniclastic breccias, volcaniclastic sandstones, 8 Middle Eocene. Calcareous
113 sandstones.
114 C - Google map with cross-section (a-b) passing the studied Malishka outcrop. Dashed line
115 shows Eocene-Oligocene boundary. U- Unconformity. Red arrows show post lower Oligocene
116 compression.
117
118 Eocene conglomerates and nummulitic limestones accumulated unconformably above all three
119 main lithotectonic units of the Lesser Caucasus: (1) Eurasian margin, (2) ophiolite nappe/suture
120 zone and (3) SAB (Sosson et al., 2010). Alkaline magmatic activity took place in the area in the
121 Middle–Late Eocene, related to post collisional extension associated with a north-dipping
122 Southern Neotethys subduction (e.g., Rezeau et al., 2017; Sahakyan et al., 2017a). In this time
123 the compressional stress-regime formed oblique-fold structures with north-dipping, NW-SE
124 oriented thrusts and reverse faults (Avagyan et al., 2018). The tectono-stratigraphic evolution
125 forced development of the Shagap piggyback basin (situated about 50 km to the west of the
126 Malishka section), which is formed by slope deposition during Middle Eocene to Oligocene time
127 (Sahakyan et al., 2017b). An upper Eocene–lower Oligocene coral reef also developed within
128 this basin (Sahakyan et al., 2020).
129 The Yeghegnadzor synclinorium includes the middle and upper basins of the Arpa River (Fig.1
130 B). The synclinorium is a large structure composed of several smaller anticlines and synclines,
131 all exhibiting a consistent SSE–NNW elongation. Upper Eocene–Oligocene sediments are found
132 in the southwest and Miocene–Pleistocene volcanic rocks in the northwest (Sargsyan, 1989). The
133 studied Malishka section is located in the Yeghegnadzor region, on the right side of the
134 Yeghegnadzor–Malishka road, at an altitude of 1249 m a.s.l (39°44'58.9"N, 45°22'28.43"E) and
135 represented by upper Eocene–lower Oligocene sediments (Fig. 1 B,C). The studied section
136 comprises a well-exposed succession of upper Eocene-Oligocene Urtsadzor and Shagap
137 formations (additional details will be discussed under lithostratigraphy and structures). The beds
138 are tilted slightly to the SSW, with a dip of 5° (Fig.1C) in the upper part and 20–30° in the lower
139 nummulitic limestones. No unconformity was identified in the field.
140
141 **3. Materials and Methods**
142 Field observations were carried out in the Malishka section based on lithology, texture, and
143 sedimentary structure, thickness of beds and nature of bed boundaries. Samples were collected

from the well-exposed outcrop (Fig. 2, 3). Structure and composition of sediments were analysed in thin sections of 30 samples (Fig. 4a, b). The facies nomenclature follows the textural classification scheme of Dunham (1962) modified by Embry and Klovan (Embry & Klovan, 1971). The quantity of carbonate grains of different types was determined visually in thin sections using Baccelle charts (Baccelle & Bosellini, 1965). CaO and MgO were analyzed in the laboratory of chemistry at the Institute of Geological Sciences following the NSAM (Research Council for analytical methods of research) guidelines (Table 1, Fig. 3).

Biostratigraphic analyses were performed on 35 samples. For the analysis of LBF, nine samples of limestone and sandstone were taken, and for the study of PF, 26 samples were collected from claystone and siltstone at approximately 1 m intervals (Figs. 3, 5). The isolated specimens of LBF were collected from weathered limestones or from underlay clays. Only isolated specimens of foraminifera were studied for species identification. The LBF were identified in equatorial sections, prepared by splitting specimens or thin sectioning. About 20 oriented thin sections of nummulitids and other larger foraminifera were prepared from free tests. The external view was also considered for species determination of *Silvestriella, Fabiania, Chapmanina,* and *Calcarina*. For identification of LBF we used the classification of Schaub (1981) for large radiate forms and *Nummulites*, Özcan et al. (2010) for reticulate *Nummulites*, Herb & Hekel (1975) for small radiate *Nummulites*, Less et al. (2008) for *Heterostegina,* Less & Özcan (2008) for *Spiroclypeus*, and the biometrical classification of Less (1998) for orthophragminids (Figs. 3, 5).

To extract tests of PF from samples, we used an optimised procedure proposed by Grigoryan & Sahakyan (2019). First, 100 g of sediment were soaked in distilled water. Then a 2% sodium pyrophosphate solution was used to cover the sample. After 48 hours, the sample was washed under running water. Then the following mixture was heated to boiling. Hard samples were boiled in 3% hydrogen peroxide solution for 30 minutes. Then samples were placed into an ultrasonic cleaner in 200 ml water at 60°C, along with 4 g sodium pyrophosphate and 6 ml hydrogen peroxide (33%) solution. Samples were washed through a sieve series with meshs sizes <63 μm, 63–200 μm, 200–500 μm, and > 500 μm. The taxonomy of PF was based on atlases by Pearson et al. (2006) and Wade et al. (2018), the biostratigraphy was based on the biozonal definitions of Berggren et al. (1995), Berggren & Pearson (2005), and Wade et al. (2011). The summarized information of identified taxonomy is presented in Table 2. Planktonic foraminiferal

tests were photographed using a scanning electron microscope (SEM) type TESCAN VEGA-II XMU in the Instrument analytics laboratory of Borissiak Palaeontological Institute of Russian Academy of Sciences, Moscow, Russia. Analyses were restricted to presence or absence of species (Figs. 6, 7).

The following acronyms for biozones and bioevents were used in this work: E – Eocene and O – Oligocene tropical/subtropical planktonic foraminiferal zones (Berggren & Pearson 2005; Wade et al., 2011), and SBZ – shallow benthic foraminiferal zones for the Tethyan Paleocene – Eocene (Serra-Kiel et al., 1998) and Oligocene (Cahuzac & Poignant, 1997). We used the LO for lowest occurrence and HO for highest occurrence datums of species.

4. Results

4.1. Sedimentology and structures

The average thickness of the Malishka section is approximately 46 m (Figs. 2, 3, 6). The lower part of the section, up to 14 m, consists of grey clayey marls and calcareous claystones, interbedded with bioclastic, brecciated limestone layers ranging from 0.05 to 0.5 m in thickness (Fig. 2B,C). Limestones are represented by extraclastic and extrabioclastic rudstones and floatstones as well as polybioclastic grain-packstones. The beds of these limestones often have sharp boundaries, featuring loading and flute casts on the bottom and erosional surfaces on the top (Fig. 2C'). Float- and rudstones commonly exhibit poor sorting of clasts and weakly expressed reverse grading in the lower part of a bed, transitioning to normal grading in the upper part. In contrast, finer-grained rocks have normal gradation. The lower coralline-nummulitic floatstone bed (Fig. 2C, samples M160, M1802) contains fragments of red algae, colonial corals, *Discocyclina* and *Nummulites* (both A and B forms) in approximately equal quantities, bryozoans, pelecypods (about 1 %) small benthic foraminifera (SBF) including miliolids and rare clasts of volcanic rocks (Figs. 3, 4a (A–C)). Microcrystalline calcite cement fills the pores between clasts, cavities and pores, comprising about 25–30% of total rock volume. In some areas the cement distribution is uneven.

The bioclasts in the sample M1600 (bioclastic floatstone) (Figs. 2, 3, 4a (D–F)) include particles of red algae, colonial and solitary corals, sponges, small orthophragminids, *Nummulites* of A and B generations, bryozoans, spines of sea urchins, rare SBF, and rare clasts of volcanic rocks.

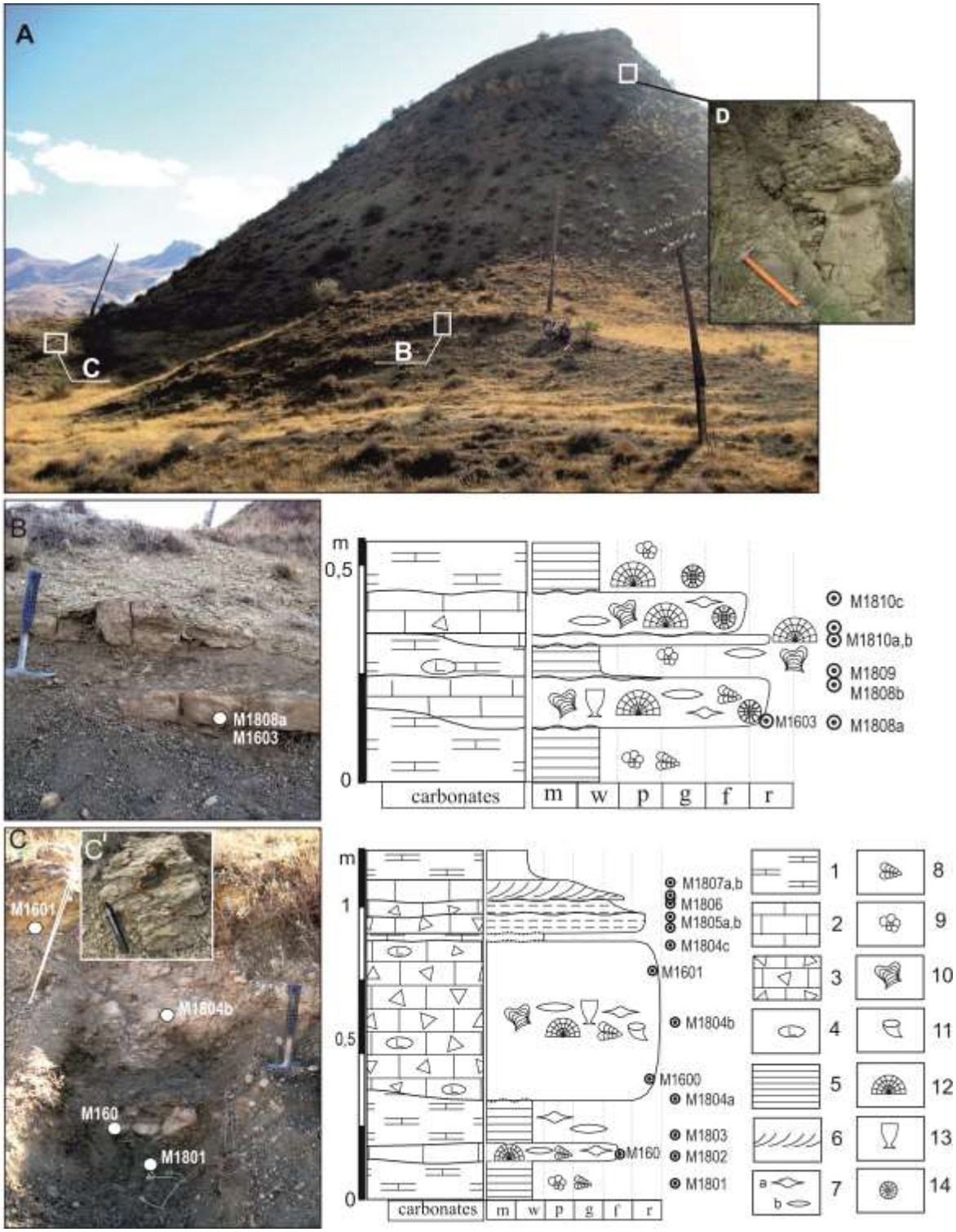


Fig. 2 Field photos of studied Malishka section. A - The common view on outcrop with indication of the Eo-Oligocene boundary; B and C - The lower part of Urtsadzor Formation. C' - volcanic rock pebbles (dot line) in limestones; D - Sandstones from upper part of Shagap Formation. 1 – marls, 2 – bioclasttic limestones, 3 – extraclastic limestones, 4 – basaltic and

limestone pebbles, 5 – parallel bedding, 6 – cross-bedding (weakly expressed structures are shown with dashed line). Bioclasts: 7 - LBF: a – orthofragminids, b – nummuliteids, 8 – smaller benthic foraminifera, 9 – planktonic foraminifera, 10 – red algae, 11 – solitary corals, 12 – colonial corals, 13 – carbonate sponges, 14 – bryozoans. Carbonates: m – mudstone, w – wackstone, p – packstone, g – grainstone, f – floatstone, r – rudstone.

The bioclasts are poorly sorted with scarce cement. The pores and cavities are filled by microcrystalline calcite. Smaller bioclastic particles vary in small size range up to 0.1–0.25 mm; larger ranges 0.5–2 mm and occasionally reaching up to 5 mm. Samples M1601, M1804(a–c) (extraclastic and extraclastic–bioclastic rudstone) contain the same types of bioclasts as in M1600. The outer walls of corallites in fragments are often encrusted with rims of coralline algae (Fig. 4b (A)). LBF make up 3–15% of rock, with orthophragminids being less common and more strongly disrupted than nummulites. Subangular to rounded extraclasts (0.5–7.4 mm and larger) are composed of different rock, ranging from peloidal to bioclastic wacke- and packstones and coralline bindstones (Fig. 4b (B)). Some peloidal limestones of extraclasts demonstrate birdseye structures (Fig. 4b (C)). In thin section, subordinate polysynthetic twinning plagioclase crystals and quartz grains (0.07-0.18 mm), along with coarse sand grains and granules of basalts, are observed. The bioclastic rudstone is overlain by marls, interbedded with two bioclastic limestone beds (Fig. 2B).

The samples M1603, M1808a, M1808b (polybioclastic floatstone) include large clasts (2-6 mm and larger) of red algae, colonial corals, pelecypods, echinoderms, sponges, small (2–4 mm) lenticular orthophragminids and *Nummulites* (A form), large (more than 8 mm) flat orthophragminids, and bryozoans (Fig. 2B). Most orthophragminid tests are broken, some *Nummulites* specimens are partially or completely dissolved and filled with drusy calcite cement, whereas small benthic foraminifera, porcelaneous inter alia, are also observed (Fig. 4a (C)). Extraclasts (about 7–10%) are composed of bioclastic and peloidal limestones with one containing a corallite fragment that features macrofaunal and microbial borings (Fig. 4b(D)). Some extraclasts are coated with crustose red algae (Fig. 4b(E)).

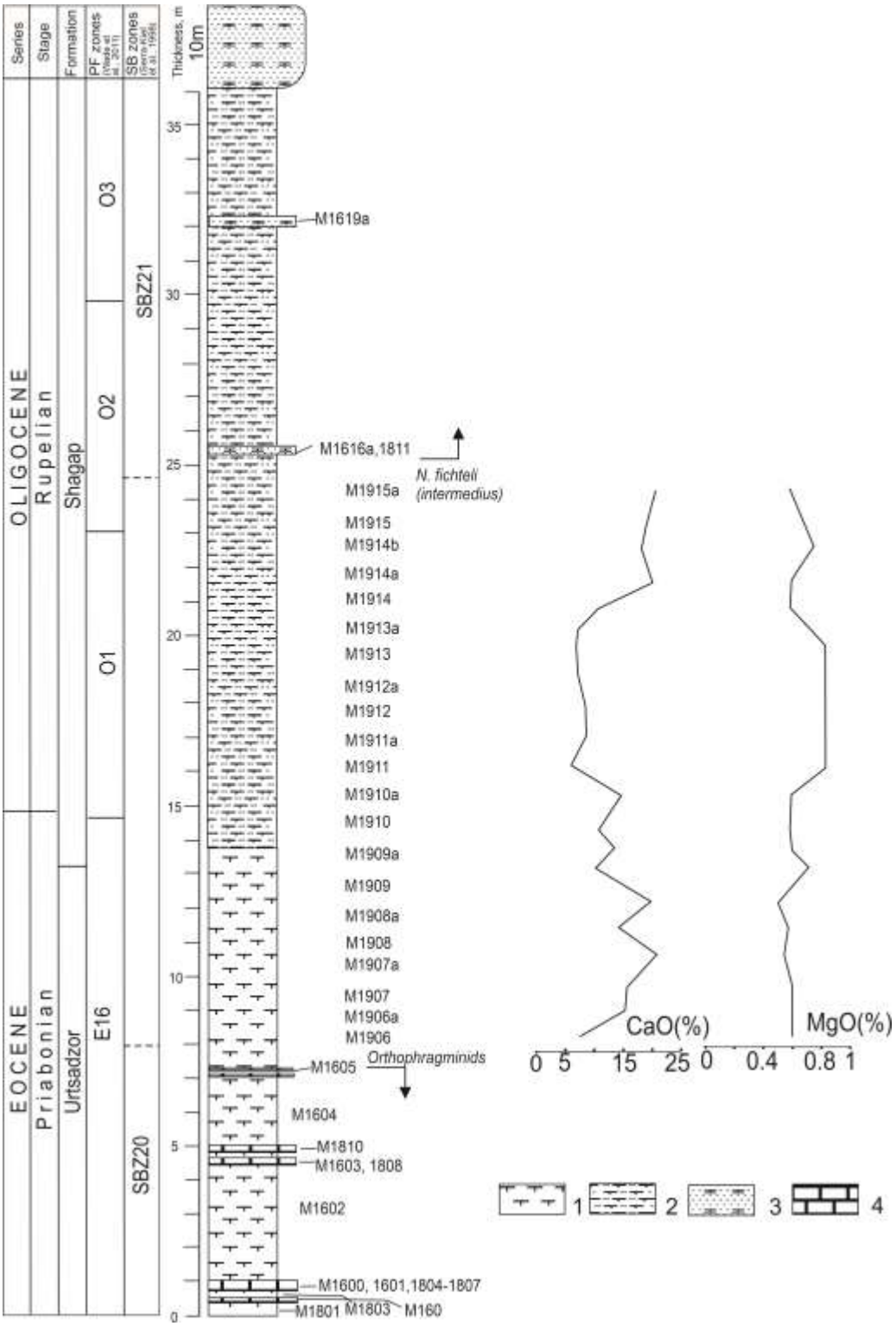


Fig. 3 Lithological logs of Urtsadzor and Shagap formations with indications of samples taken from 2016-2018 and the distribution of CaO and MgO concentration (%) across the Eocene-Oligocene boundary in Malishka section. 1.-Marls, 2.- Clay-siltstone, 3-Sandstone, 4-Limestone.

Clasts are randomly arranged, with the average size of fragments of colonial corals, commonly encrusted with coralline algae, varying from 1mm to 0.1–0.25 mm (Fig. 4a (H.I)). Large carbonate grains (15-40%) are surrounded by smaller bioclasts (less than 2 mm) in micrite and middle crystalline calcite cement of basal and porous types. Individual quartz grains and plagioclase crystals are visible in the pelitic cement.

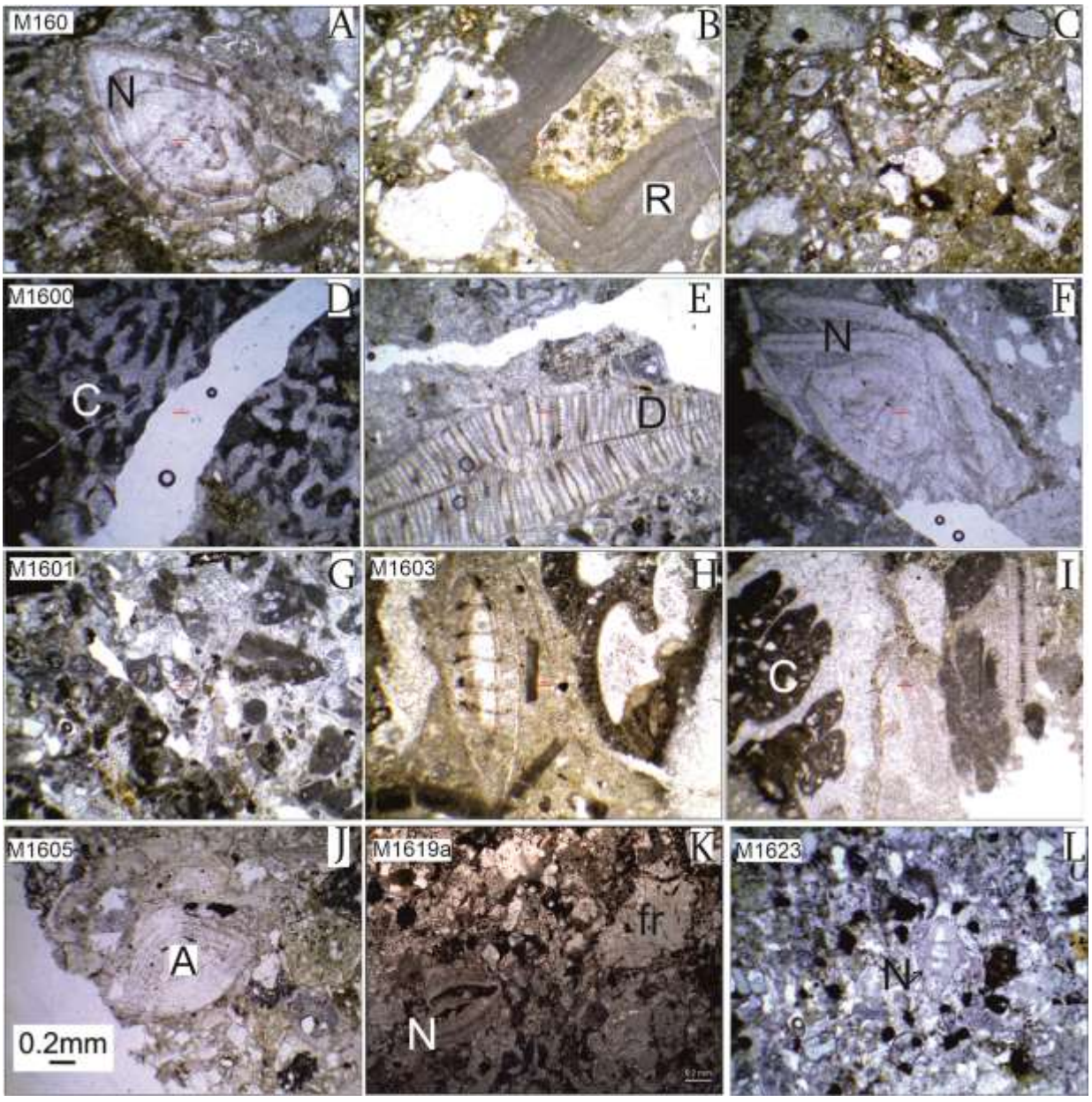


Fig. 4a Representative thin section photomicrographs from the Malishka section Observations are under parallel nicols all at the same scale (0.2 mm). R – Red algae-thallus; C – Colonial corals; D – Discocyclina; N – Nummulite; A – Asterigerinids, Q – Quartz; fr – Rock fragment.

Large grains of floatstones (2-10 mm and more, 20-40%) in the upper floatstone interbed (Fig. 2C, M1810 a–c) consist of clasts of colonial corals, with subordinate fragments of large flat and saddle-shaped nummulitids, flat orthophragminids and extraclasts of peloidal packstones. These grains, like the corals, are sometimes encrusted with coralline algae (Fig. 4b (E)). Among the smaller bioclasts (1-2 mm), lenticular *Nummulites* and orthophragminids are present with a minor abundance of *Nummulites*.

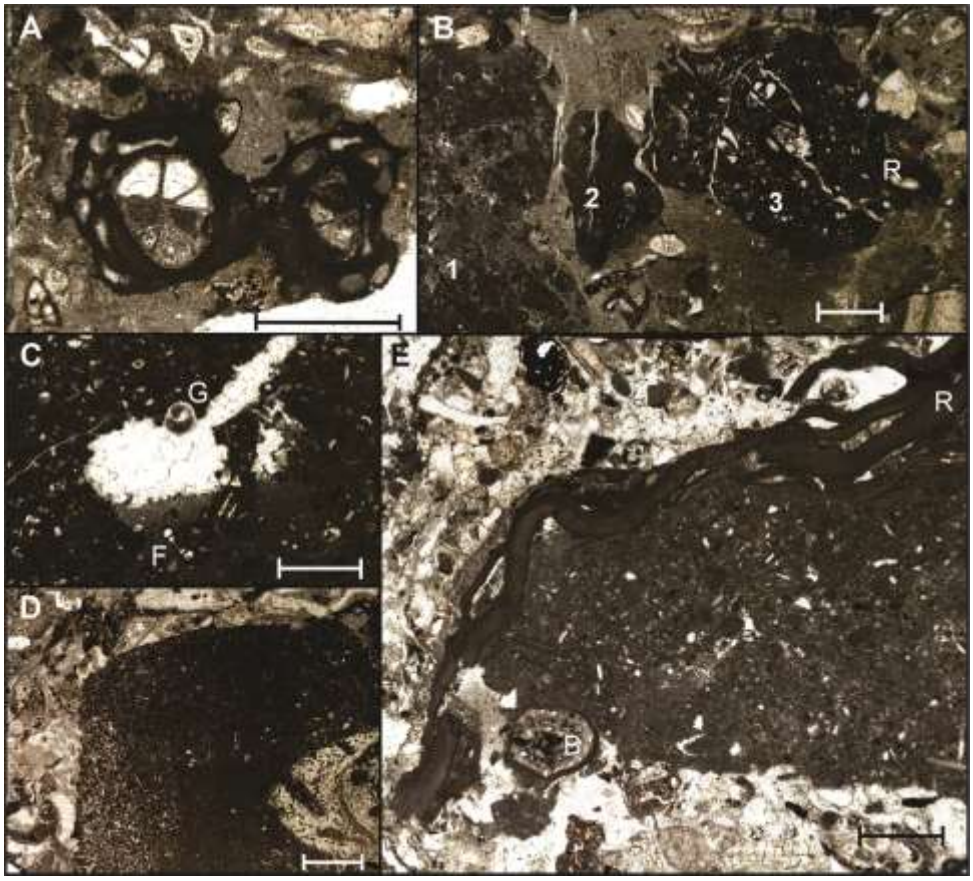


Fig. 4b Microfotographs of coated grains and extraclasts of Urtsadzor formation in Malishka section. **A** – Bioclastic-extraclastic rudstone (M1804a, Fig.2B). Red algae encrust corallites. **B** – Bioclastic-extraclastic rudstone (M1804a). Subrounded to subangular extraclasts are composed of: 1 – microbial fine-clotted peloidal packstons; 2 – coralline bindstone; 3 – peloidal-bioclastic packstone, with SBF tests and coralline algae clast (R). **C** – Bioclastic-extraclastic rudstone (M1804a). Fabric of an extraclast. Fenestrae with internal peloidal sediments with SBF (F) in microbial peloidal wackestone with juvenile gastropod shell (G). **D** – Bioclastic rudstone (M1808b, Fig.2C). Rounded extraclast composed of microbial peloidal packstone and grainstone includes bioeroded corallite. **E** – Extraclastic-polybioclastic rudstone (M1810b, Fig.2C m). Peloidal packstone with fine carbonate debris extraclast was coated with crustose coralline algae and then broken during resedimentation. Scale bar length 1 mm.

The nummulitic sandy limestone (Fig. 3, sample M1605) contains up to 10 cm in diameter volcanic and carbonate rock pebbles (Fig. 2C'). Red algae (biopellets) are not well preserved. Asterigerinids and other SBF are also present (Fig. 4a (J)). The cements in the sample are porous microcrystalline calcite. Non-carbonate components of the rock make up 25%, consisting of plagioclase, angular to semi-rounded quartz grains, as well as minerals like hydroxide iron, amphibole, and magnetite.The middle part of the section, representing the Shagap Formation, contains calcareous clays and siltstones which contain numerous planktonic foraminifera and SBF. LBF are scare, with only about 10 tests observe. Sample M1619a (Figs. 3, 4a (K)) is an indurated brown-grey rock consisting of a poorly sorted heterogeneous mixture. This includes volcanic and limestone rock fragments, angular polysynthetic twinning plagioclase, quartz grains of sand size, volcanic glass, and magnetite, which all are embedded in a mud matrix. Bioclasts include rare fragments of broken *Nummulites* (Fig.4a (K)), pelecypods, bivalves, gasteropods and bryozoans. Most of the upper part of the section (ca. 10 m) is dominated by middle- to coarse-grained quartz-plagioclase sandstones (samples M1620–1623 in Fig. 3). These sandstones are composed of quartz and plagioclase grains, volcanic glass, amphibole, muscovite minerals, and fragments of limestone and volcanic rocks. Iron oxide concretions coat the surfaces of quartz grains. Coarse-grained sandstone (sample M1623) occasionally includes small *Nummulites* (Fig. 4a (L)).

To evaluate weathering conditions at the time of deposition, the CaO and MgO contents, along with the MgO/CaO ratio as an indicator of chemical alteration, were analyzed in claystones and siltstones (Table 1, Fig. 3, samples 1906-1915a). The MgO content ranges from 0.32% to 0.5%. It appears relatively consistent across the different levels, with no dramatic changes, though there is a slight increase in MgO content around the 16–20.2 m interval. The CaO content varies widely, from 4.19 to 14.83%. The highest CaO contents were found in the samples M1914a (14.25%) and M1915a (14.23%), at the level of 21.8 to 24.2 m. The MgO/CaO ratio is relatively high, ranging from 0.12 to 0.08 in samples M1911–1913a.

Table 1 MgO, CaO and Mg/Ca composition of sediments from various depth

Level in section (m)	samples	MgO (%)	CaO (%)	MgO/CaO (%)
8	M1906	0.36	5.21	0.07
8.9	M1906a	0.36	10.95	0.03
9.3	M1907	0.36	11.11	0.03
10.2	M1907a	0.32	14.83	0.02
11	M1908	0.35	10.01	0.03
11.7	M1908a	0.33	14.06	0.02
12.6	M1909	0.45	7.29	0.06
13.7	M1909a	0.36	9.52	0.04
14.5	M1910	0.35	7.55	0.05
15.2	M1910a	0.35	10.34	0.03
16.1	M1911	0.5	4.19	0.12
16.8	M1911a	0.5	6.09	0.08
17.7	M1912	0.5	6.18	0.08
18.8	M1912a	0.5	5.29	0.09
19.8	M1913	0.5	4.87	0.10
20.2	M1913a	0.5	4.87	0.10
20.8	M1914	0.36	7.53	0.05
21.8	M1914a	0.35	14.25	0.02
22.6	M1914b	0.39	12.9	0.03
23.2	M1915	0.45	13.6	0.03
24.2	M1915a	0.36	14.23	0.03

4.2. Larger bentic foraminiferal stratigraphy

In the Malishka section (Fig. 3), LBF are dominated by poorly preserved nummulitids (genera *Nummulites, Operculina, Heterostegina, Spiroclypeus*), pellatispirids (genus *Pellatispira*) and orthophragminids. The upper Eocene LBF are diverse (Fig. 5a, b), but distributed unevenly along the layer (Fig. 4a). Both A and B generations of nummulitids and orthophragminids are present in the sediments of the lower part of outcrop. However, it is difficult to count the A/B ratio because of incomplete tests and mode of tests sampling under limestones.

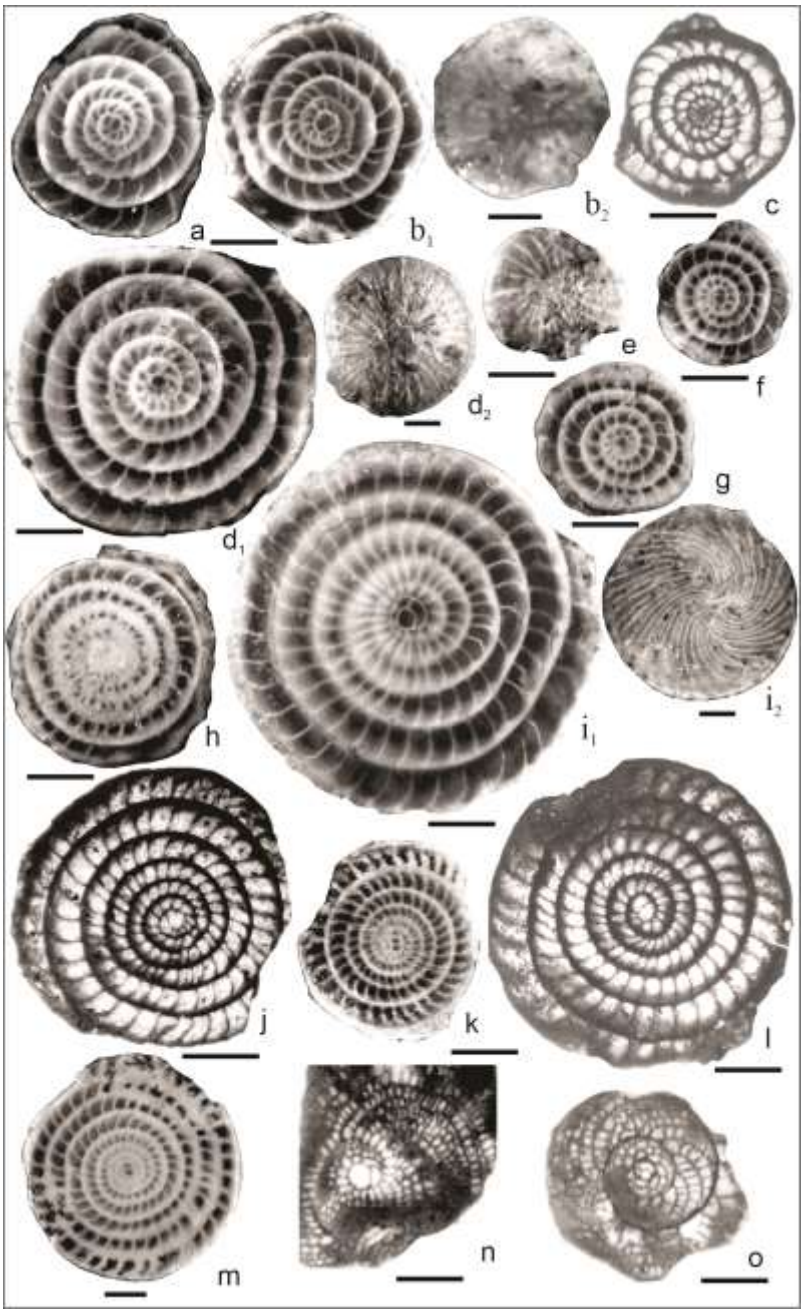


Fig. 5a Zonal and characteristic radiate *Nummulites* and *Heterostegininae* from the Malishka section. a-c: *N. vascus* Joly & Leymerie (sample M1619a), $d_{1,2}$: *N aff. Vascus* (sample M1619a); e-h: *N. incrassatus* de la Harpe, e-g (sample M1619a), h (sample M1616a); $i_{1,2}$-j: *N. striatus* (Bruguière), $i_{1,2}$ (sample M1810), j (sample M1619a); k: *N. beaumonti* d'Arch. et Haime (sample M1809); m: *N. vicaryi* d'Arch. et Haime; n: *Heterostegina gracilis* Herb (sample M1805); o: *Spiroclypeus carpaticus* (Uhlig) (sample M1810). A generation (a, b_1, d_1, f, g, h, i_1, j); B generation (c, h); equatorial sections (k-o); surfaces (b_2, d_2, e, i_2). Scale bar – 1 mm.

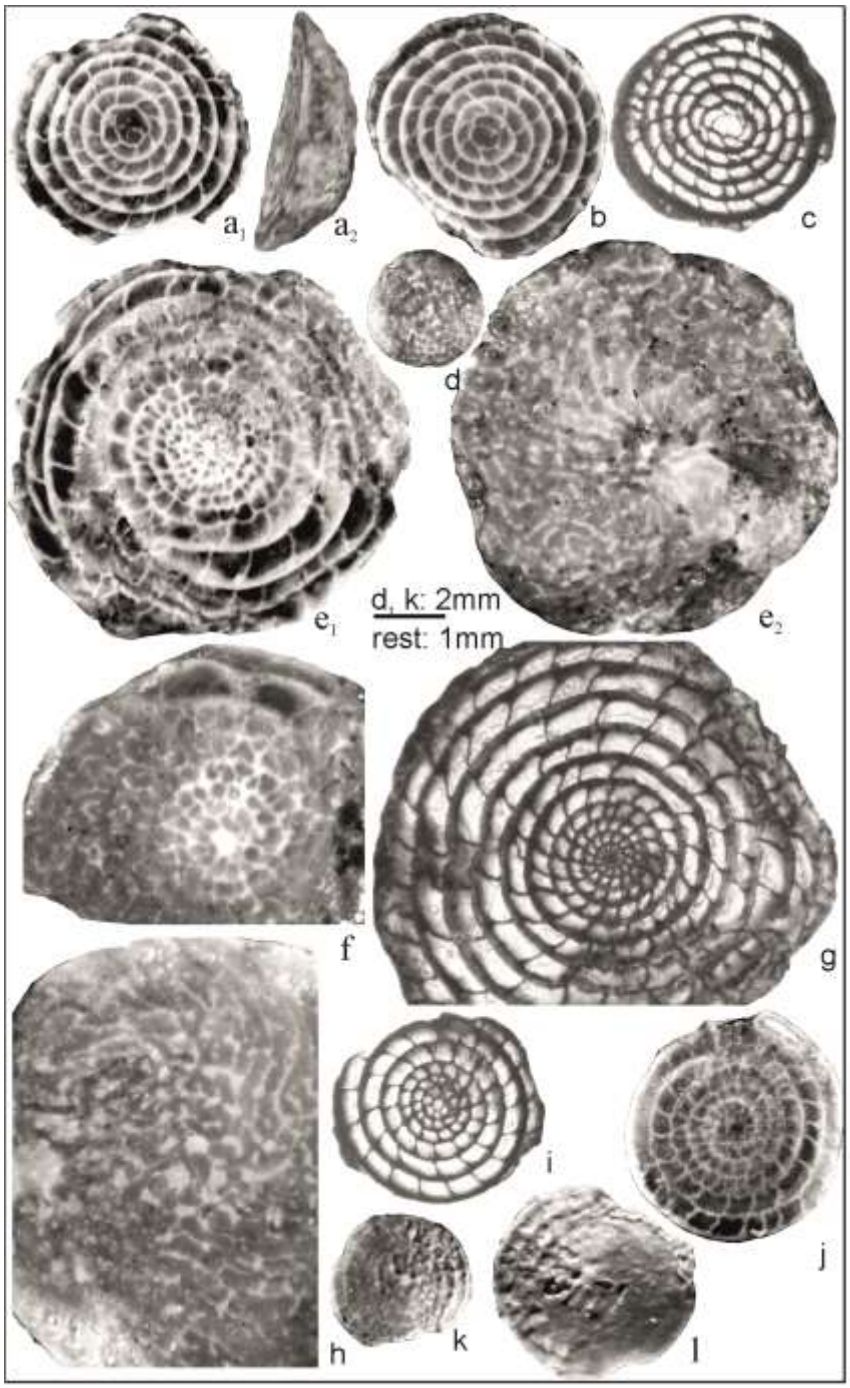


Fig. 5b Reticulate Nummulites from the Malishka section. **a-f:** *N. fichteli* Michelotti (sample M1619a); g-i: *N. fabianii* (Prever), g (sample M1810), h (sample 1601), i (sample M1619a), j,l (sample M1805), k (sample M1804); A generation (a-d, i-l); B generation (e-h); equatorial sections (a, b, c, e_1, g_1, l, j); surfaces (f-polished, a_2-side view). Scale bar – 1 mm.

The most common taxa (10-50 tests) among LBF are the small *Nummulites* (*N. incrassatus*, *N. fabianii*). The LBF are especially rich in the middle and upper interlayers of the bio-lithoclastic carbonate facies from the lower part of the outcrop (Figs. 2B; samples M1804a, M1601, M1805a, b). The LBFs of these limestones are represented by *Nummulites incrassatus*, *N. variolarius, N. striatus* and reticulate *Nummulites fabianii* Prever (A and B generations), scarce *Assilina alpina*, *Heterostegina gracilis*, as well as individual orthophragminids: *Orbitoclypeus zitteli*, *Discocyclina dispansa*, and *Asterocyclina* sp. We recognized *N. fabianii, N. striatus*, *N. stellatus*, *N. bouillei*, *Spiroclypeus* sp., *Orbitoclypeus varians varians, Pellatispira madaraszi*, and *Asterocyclina stella* in limestones situated 3 m above (Fig. 3, samples M1603, M1810). The third layer of limestone contains rare nummulitids and other LBF, is 0.1–0.3 m in thickness, and is situated in 2–2.2 m above. The most important nummulitids of this layer (sample M1605) include *N. fabianii* and a single *H. gracilis*. The other LBF, distributed in upper Priabonian facies, are represented by *Calcarina* sp., *Chapmanina* sp., *Sphaerogypsina globula* , and *Halkyardia minima* (Fig. 3).

The Oligocene LBFs are rare (fewer than 10 tests of a single species per sample) and are represented by a single genus, *Nummulites*, corresponding to SBZ21. About 15 tests were extracted from sample M1616a and 30 tests from sample M1619a, both with dimensions of 10 × 12 × 3 cm. The stratigraphically lowest level with LBF (sample M1616a) contains the following taxa such as *N. vascus, N. fichteli* , scarce *N. incrassatus* (Fig. 5a, b) and *N.* cf. *bouillei*. Overlaid carbonate greywacke (sample M1619a) consists of common oysters, pectenids, corals, ostracods, SBF and *Nummulites*. The last are represented by *N. fichteli* and *N. vascus,* characteristic for Rupelian, as well as *N.* cf. *striatus* close to upper Eocene (Fig. 5a, b). Reticulate *Nummulites* from the Malishka section are represented by *N. fichteli* Michelotti (A and B generation) and *N. fabianii* (Prever) from various samples (Fig. 5b).

4.3. Planktonic foraminiferal biostratigraphy

The ranges of planktonic foraminiferal species (Table 2) are summarized in Figure 6, and details of their microtexture and structure are illustrated in Figure 7a-c.

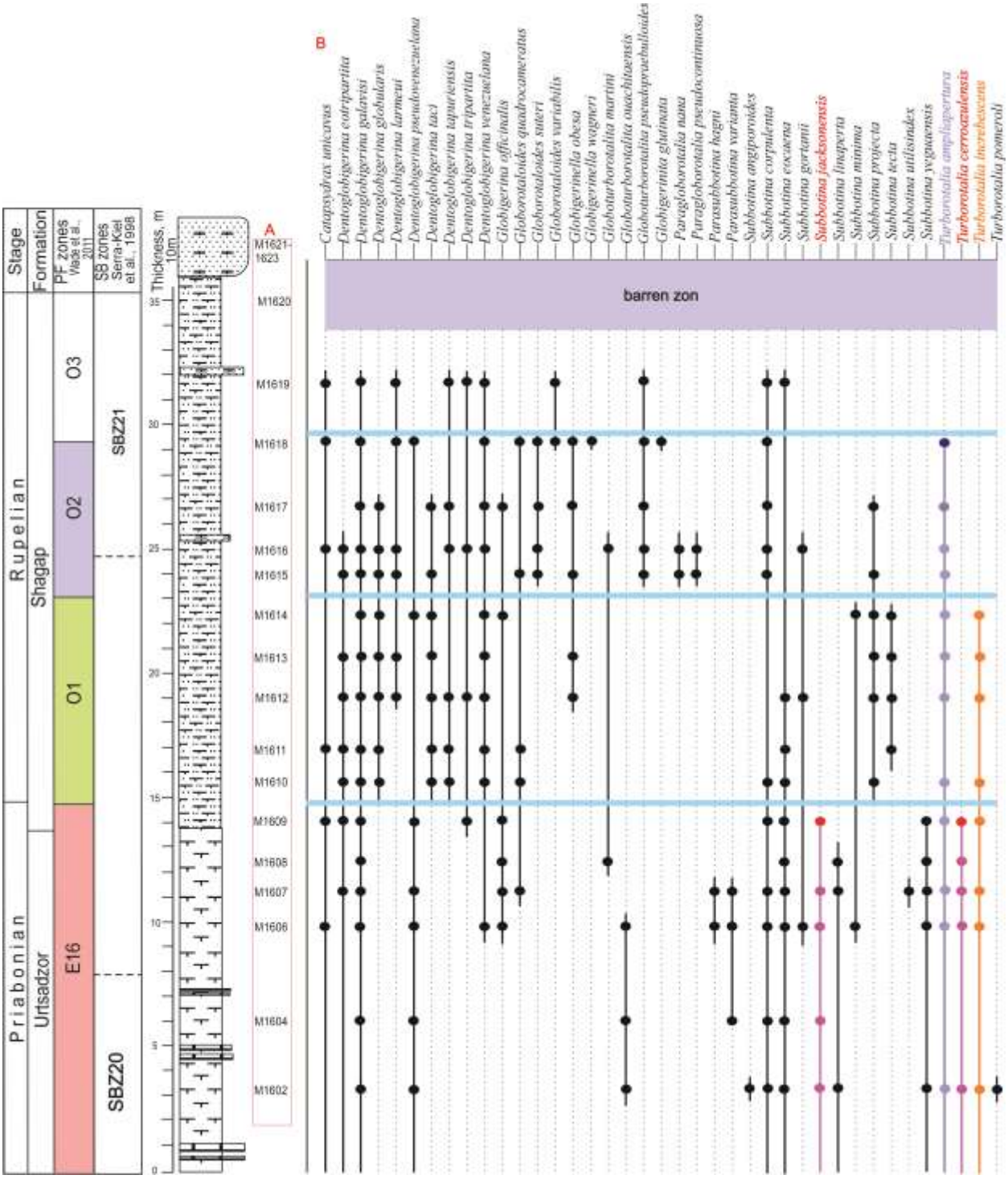


Fig. 6 Occurrences of planktonic foraminiferal in the Malishka section with indication of A - micropaleontological samples, B - PF species range. Lines show interpolation between observed occurrences (dots).

359 **Table 2** Planktonic foraminiferal assemblages of Malishka Section. Samples M1602-M1609
360 correspond to the assemblage 1, samples M1610-1620 to assemblage 2.
361

Species	samples	Assemblages
Catapsydrax unicavus (Loeblich & Tappan, 1957)	M1606-1619	1 & 2
Dentoglobigerina eotripartita (Olsson et al., 2006)	M1602-1619	1 & 2
Dentoglobigerina galavisi (Bermudez, 1961)	M1602-1619	1 & 2
Dentoglobigerina globularis (Bermúdez, 1961)	M1610-1617	2
Dentoglobigerina larmeui (Akers, 1955)	M1612-1618	2
Dentoglobigerina pseudovenezuelana (Blow and Banner, 1962)	M1602-1618	1 & 2
Dentoglobigerina taci (Pearson & Wade, 2015)	M1610-1617	2
Dentoglobigerina tapuriensis (Blow & Banner, 1962)	M1610-1619	2
Dentoglobigerina tripartita (Koch, 1926)	M1609-1619	1 & 2
Dentoglobigerina venezuelana (Hedberg, 1937)	M1606-1619	1 & 2
Globigerina officinalis (Subbotina, 1953)	M1606-1617	1 & 2
Globorotaloides quadrocameratus (Olsson et al., 2006)	M1607-1618	1 & 2
Globorotaloides suteri (Bolli, 1957)	M1615-1618	2
Globorotaloides variabilis (Bolli, 1957)	M1618,1619	2
Globigerinella obesa (Bolli, 1957)	M1612-1618	2
Globigerinella wagneri (Rögl, 1994)	M1618	2
Globoturborotalita martini (Blow & Banner, 1962)	M1608,1616	1 & 2
Globoturborotalita ouachitaensis (Howe & Wallace ,1932)	M1602-1606	1
Globoturborotalita pseudopraebulloides (Spezzaferri et al., 2018)	M1615-1619	2
Globigerinita glutinata (Egger, 1893)	M1618	2
Paragloborotalia nana (Bolli 1957)	M1615,1616	2
Paragloborotalia pseudocontinuosa (Jenkins, 1967)	M1615,1616	2
Parasubbotina hagni (Gohrbandt, 1967)	M1606,1607	1
Parasubbotina varianta (Subbotina, 1953)	M1604-1607	1
Subbotina angiporoides (Hornibrook,1965)	M1602	1
Subbotina corpulenta (Subbotina, 1953)	M1602-1619	1 & 2
Subbotina eocaena (Guembel, 1868)	M1602-1619	1 & 2
Subbotina gortanii (Borsetti, 1959)	M1606-1616	1 & 2
Subbotina jacksonensis (Bandy 1949)	M1602-1609	1
Subbotina linaperta (Finlay 1939)	M1602-1608	1
Subbotina minima (Jenkins, 1966)	M1606-1615	1 & 2
Subbotina projecta (Olsson et al., 2018)	M1610-1617	2
Subbotina tecta (Pearson & Wade, 2015)	M1611-1614	2
Subbotina utilisindex (Jenkins & Orr, 1973)	M1607	1
Subbotina yeguaensis (Weinzierl & Applin, 1929)	M1602-1609	1
Turborotalia ampliapertura (Bolli, 1957)	M1602-1619	1 & 2
Turborotalia cerroazulensis (Cole, 1928)	M1602-1609	1
Turborotalia increbescens (Bandy, 1949)	M1606-1614	1 & 2
Turborotalia pomeroli (Toumarkine & Bolli, 1970)	M1602	1

362

363 The lower part of the section (samples M1602–M1609) is characterized by a diverse assemblage
364 of foraminiferal species. Some taxa (*Dentoglobigerina galavisi, D. pseudovenezuelana,*

Subbotina corpulenta, S. eocaena, Turborotalia ampliapertura) show continuous distribution upwards, while others (*Subbotina angiporoides, Turborotalia pomeroli*) are restricted to this lower zone. The zonal marker *Hantkenina alabamensis* was not identified in the studied samples. The highest occurrence (HO) of *Turborotalia cerroazulensis* is observed at ~ 15 m. The LO of *Dentoglobigerina tripartita* and *D. venezuelana* appear between 10 and 15 m, while the LO of *Globigerinella obesa* is recorded around 19 m. The LO of *Dentoglobigerina taci* and *Subbotina tecta* are observed at ~ 15–17 m, respectively. *Subbotina tecta* persists throughout this interval, with its HO recorded at the top (~ 23 m). The 15–25 m interval of the section exhibits high diversity and frequency of foraminiferal species. *Turborotalia increbescens* reaches its HO at ~ 23 m. The foraminiferal record remains diverse, with the LO of *Globoturborotalita pseudopraebulloides, Globorotaloides suteri, Paragloborotalia pseudocontinuosa,* and *P. nana* at approximately 24 m. *Turborotalia ampliapertura* reaches its HO at the top of the section (~30 m). A barren zone characterizes the upper section (~35–40 m).

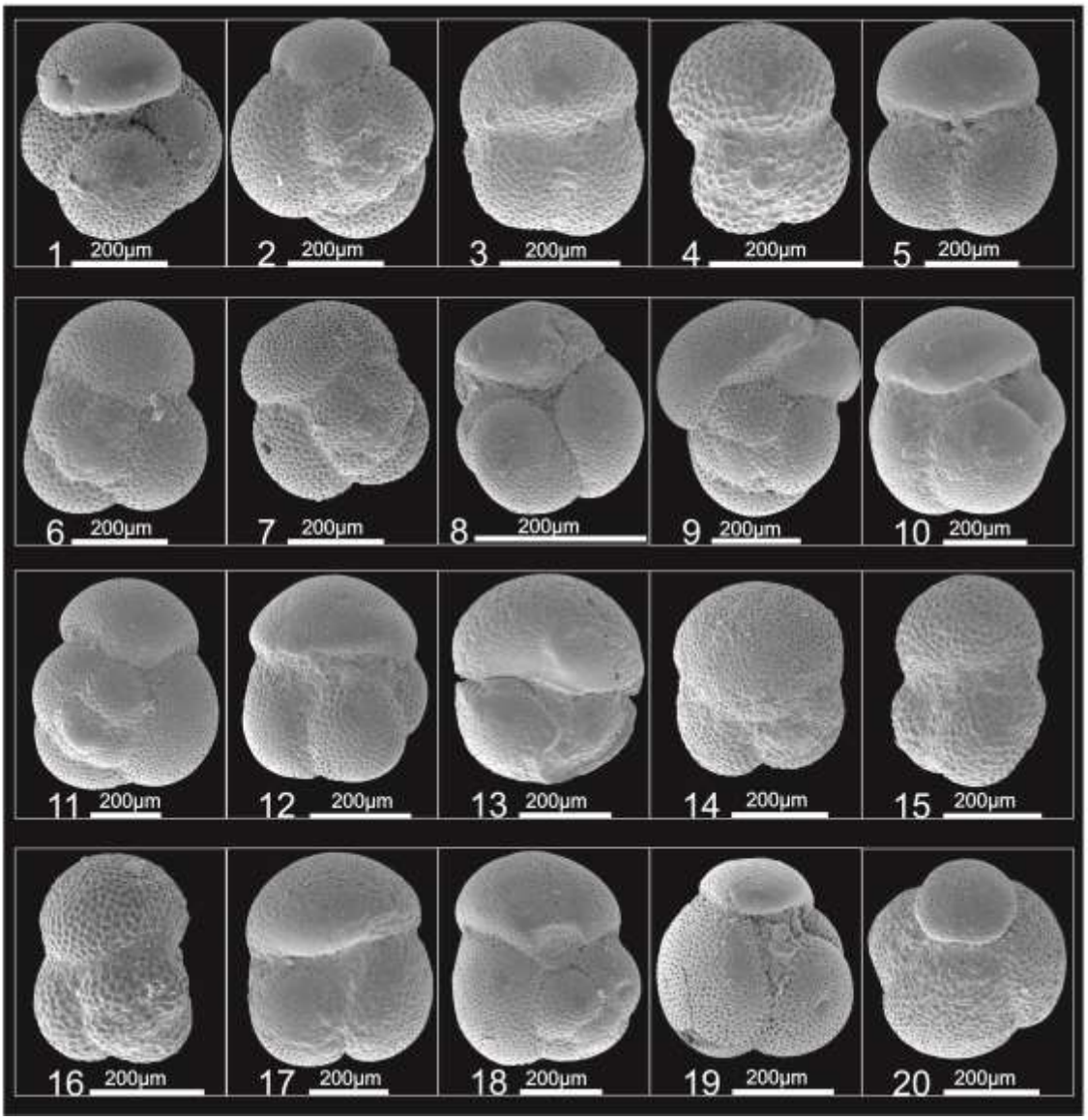


Fig. 7a Scanning Electron Microscopy of planktonic foraminifera from the Malishka section. 1-2. *Dentoglobigerina baroemoenensis*, sample M1616 (1 umbilical view, 2 spiral view) , 3-4. *Dentoglobigerina eotripartita*, sample M1612 (3 umbilical view, 4 spiral view), 5-6. *Dentoglobigerina galavisi*, sample M1614 (5 umbilical view, 6 spiral view), 7. *Dentoglobigerina globularis,* sample M1610 (spiral view), 8-9 *Dentoglobigerina larmeui,* sample M1618 (8 umbilical view, 9 spiral view), 10-11. *Dentoglobigerina prasaepis*, sample M1615 (10 umbilical view, 11 spiral view), 12. *Dentoglobigerina pseudovenezuelan*, sample M1613 (umbilical view), 13-14. *Dentoglobigerina sellii*, sample M1617 (13 umbilical view, 14 spiral view), 15-16. *Dentoglobigerina taci*, sample M1610 (15 umbilical view, 16 spiral view), 17-18. *Dentoglobigerina tapuriensis*, sample M1610 (17 umbilical view, 18 spiral view), 19. *Dentoglobigerina tripartite*, M1611 (umbilical view), 20. *Dentoglobigerina venezuelana*, sample M1612 (20 umbilical view, 21 spiral view).

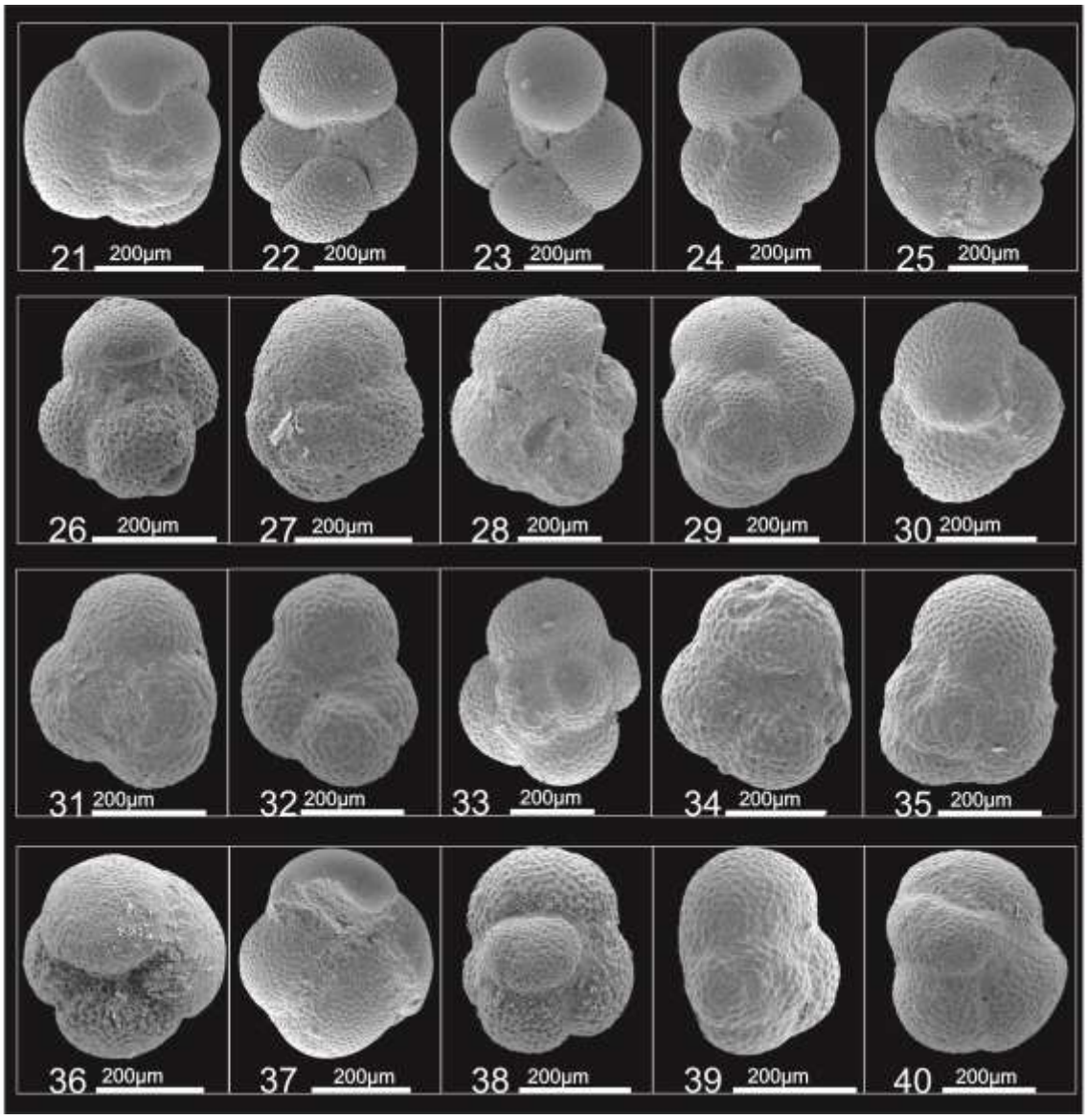


Fig. 7b Scanning Electron Microscopy of planktonic foraminifera from the Malishka section. 21. *Dentoglobigerina venezuelana*, sample M1612 (20 umbilical view, 21 spiral view), 22. *Globigerinella obesa*, sample M1613 (umbilical view), 23. *Globigerinella wagneri*, sample M1616 (umbilical view), 24. *Globoturborotalita pseudopraebulloides*, sample M1615 (umbilical view), 25. *Paragloborotalia nana*, sample M1616 (umbilical view). 26-27. *Parasubbotina hagni*, sample M1607 (26 umbilical view, 27 spiral view), 28-29. *Parasubbotina varianta*, sample M1614 (28 umbilical view, 29 spiral view), 30-31. *Subbotina corpulenta*, sample M1602 (30 umbilical view, 31 spiral view), 32-33. *Subbotina corpulenta*, sample M1604 (32 umbilical view, 33 spiral view), 34-35. *Subbotina eocaena*, sample M1606 (34 umbilical view, 35 spiral view), 36-37. *Subbotina gortanii*, sample M1612 (umbilical view), 38-40. *Subbotina jacksonensis,* sample M1609 (38,40,42 umbilical view, 39,41 spiral view).

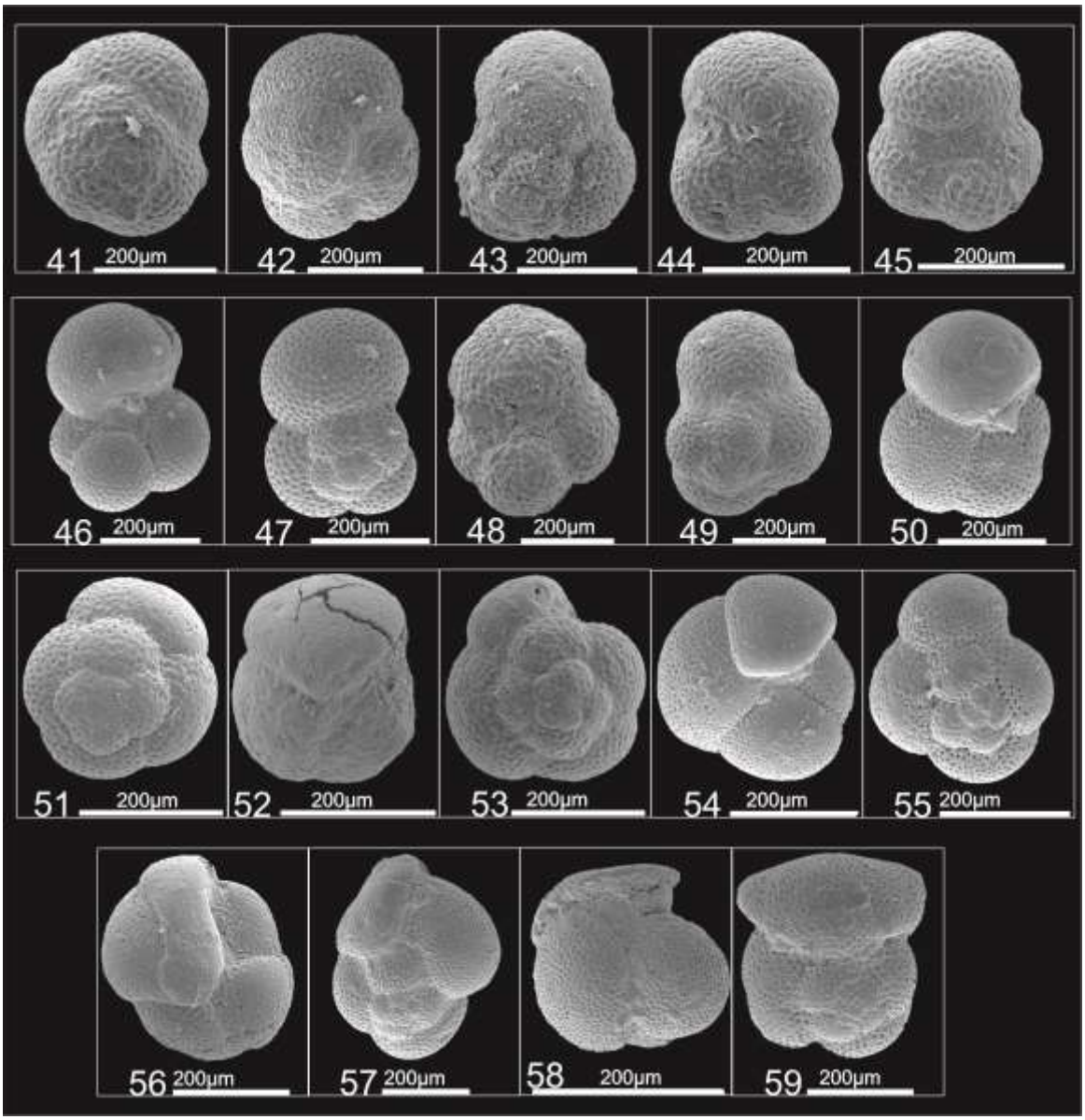


Fig. 7c Scanning Electron Microscopy of planktonic foraminifera from the Malishka section. 41. *Subbotina jacksonensis,* sample M1609 (38,40,42 umbilical view, 39,41 spiral view), 43-44. *Subbotina linaperta*, sample M1608 (44 umbilical view, 43 spiral view), 45-47. *Subbotina tecta,* sample M1612 (45, 46 umbilical view, 47 spiral view), 48-49. *Subbotina yeguaensis*, sample M1607 (48 umbilical view, 49 spiral view), 50. *Turborotalia ampliapertura*, (sample M1613 umbilical view). 51. *Turborotalia ampliapertura*, sample M1613 (spiral view), 52-53. *Turborotalia cerroazulensis*, sample M1609 (52 umbilical view, 53 spiral view), 54-55 *Turborotalia increbescens*, sample M1614 (54 umbilical view, 55 spiral view), 56-57. *Turborotalita praequinqueloba*, sample M1611 (56 umbilical view, 57 spiral view), 58-59. *Dent* sp., sample M1612 (58 umbilical view, 59 spiral view).

5. Discussion

5.1. Depositional environment

The studied Malishka section is dominated by clay to carbonate lithofacies, including extraclastic and extra-bioclastic rudstones and floatstones, as well as grain-packstones in the lower parts. The transition from clay-siltstones in the middle section to sandstones in the uppermost parts suggests a shift in depositional environment and energy conditions over time. In the lowermost part of the section, clayey marls and calcareous clays contain numerous PF and SBF with scarce LBF, indicate a quiet, relatively deep outer shelf or distal ramp paleoenvironment. However, the composition and structure of carbonate grains in limestones demonstrate signs of different conditions of their origin. Most of bioclasts in limestones: LBF and SBF, solitary and colonial corals, red algae, echinoderms, bryozoans, bivalves and rare carbonate sponges, mixed with coarse clastics, indicate transport from a shallower-shelf euphotic zone. Widespread crusts of coralline algae upon colonial corals (Fig. 4b) and carbonate particles of other genesis (Fig. 4b) were marked as a feature of high-energy conditions of Cenozoic reefs (Bosence, 1983; Bosence, 1985; Brasier & Donahue, 1985; Reading et al., 1996; Tucker & Write, 1990). Microbial fine-peloidal fabrics of many intraclasts indicate formation in low-energy lagoonal to intertidal conditions (Flügel, 2004). The presence of porcelaneous Miliolida tests is commonly associated with environments characterized by restricted water-mass exchange (Papazzoni, Trevisani, 2006; Mateu-Vicens et al., 2012; Hadi et al., 2016). Flattened tests of nummulitids and orthophragminids are assumed to indicate deeper environments compared to LBF with lenticular tests (Aigner, 1983). Rounded and well-rounded pebbles of basalt were transported from the deltaic or beach (preferably, for small amounts of sand-sized clastics) in the coastal zone of volcanic land. The co-location and mixture of these grains with coarse clastics in limestone beds may result from high-energy, storm-generated currents, which transported material from facies zones of varying depths and hydrodynamic conditions. However, the variation in bioclastic composition across different beds indicates that storms disturbed various facies zones. The lowermost thin limestone bed, rich in nummulitids and fragments of colonial corals, likely formed from material transported from a reef front and potential nummulite bank(s). The next, thicker bed, containing numerous extraclasts of bioclastic and peloidal packstones, as well as pebbles of volcanic rocks, suggests a stronger disturbance that also affected the shoreline and

back-reef lagoon. The structure of limestone beds provides insight into material transport processes. Floatstones and rudstones are typically poorly sorted, showing weakly expressed reverse grading in the lower part of a bed, transitioning to normal grading in the upper part. In contrast, finer-grained rocks generally exhibit normal grading. The coarse bioclastic and extraclastic material was transported by grain flows, while most of the sand-sized material was likely carried by diluted turbidity currents. These currents formed interbeds with parallel and cross lamination (Fig. 2). Flute casts at the base of the carbonate beds in the section were formed by erosional marks cut by gravity-driven currents. Unfortunately, the weakly expressed structures and intense jointing hindered the restoration of the flow direction. Diversity and proximity of upper-slope facies zones are expected under ramp conditions, making the ramp the most likely sedimentary model for the shoreline of a volcanic land. Ramp model is supported by presence of non-carbonate pebbles in limestone beds, indicating the absence of a substantial barrier between the shoreface and the offshore-transition zone. This is more characteristic of ramp systems (Reading et al., 1996) and aligns with the general transport mechanism of sedimentary fabrics formed by high-energy gravity-driven currents. Limestone beds exhibit sharp and eroded surfaces on the top (Fig. 2B′), interpreted as the result of partial sediment rewashing and removal by intense currents. This suggests that the hydrodynamics of uppermost Eocene sedimentation ranged from quiet to very active environmental conditions. The most probable depth of accumulation for the Malishka section sediments was near the mean storm wave base. The increase in clastic (polymictic) influx and the reduction of shallow-shelf-produced bioclasts near the Eocene–Oligocene transition in the Malishka section mark a phase of tectonic activation in the region and the destruction of shallow-shelf biotic communities. Greywackes in the lower Oligocene (sample M1619a, X m) could have also been produced by submarine landslides, massive slumping, or dense, sediment-laden, gravity-driven turbidity flows.

A slight increase in MgO content between the 16–20.2 m interval could indicate minor fluctuations, reflecting localized changes in depositional or environmental conditions. The elevated CaO values between 21.8 m and 24.2 m suggest a higher degree of calcium carbonate precipitation during this period, likely due to changes in water chemistry or the depositional environment. MgO/CaO paleothermometry suggests that the incorporation of magnesium in

476 calcite precipitated from seawater is temperature-dependent (Evans et al., 2018). The elevated
477 MgO/CaO ratio (0.08–0.12) in samples M1911–M1913a (Fig. 3) may also provide insights into
478 past climate conditions during sediment deposition.
479
480 **5.2. Foraminifera assemblage: Paleoenvironment, biostratigraphy**
481
482 Besides the Malishka section, diverse shallow-water biota from the upper Priabonian–lower
483 Rupelian are also present in other areas. The Priabonian shallow-water paleobiocenosis of the
484 Malishka section is distinguished by the abundant presence of coralline red algae in rhodolites
485 and encrusting forms, as well as a greater diversity of corals. These differences are likely due to
486 the isolation of the piggyback basin during the Eocene (Sahakyan et al., 2017b). However, while
487 the Eocene LBF assemblages are similar (Zakrevskaya et al., 2014), the Oligocene LBF
488 assemblages exhibit distinct differences compared to those from other sections of Armenia. The
489 presence of *N. fabianii* and *H. gracilis* in sample M1605 indicates a Late Eocene (Priabonian)
490 age and suggests deposition in a warm, shallow marine environment. The presence of other LBF
491 in the upper Priabonian facies such as *Calcarina* sp., *Chapmanina* sp., *Sphaerogypsina globula*,
492 and *Halkyardia minima* indicates a diverse assemblage characteristic of this time interval.
493 Two common species of the lowest Oligocene in the other sections and the Malishka section are
494 *Nummulites vascus* and *N. bouillei*. In addition to the typical Oligocene *Operculina complanata*
495 and *N. vascus*, the rare Eocene Discocyclina and Orbitoclypeus are present in the lower
496 Rupelian.At the same time *N.* cf. *striatus* is present in the nummulitic assemblage of the lower
497 Rupelian in the Malishka section. *N. striatus* possesses radiate septal filaments, which the traces
498 appear on the test surface as “straight or curved lines marking the chamber junctions” (Adams,
499 1988). The traces of filaments are more or less curved in the Priabonian *N. striatus* from
500 Malishka, as well as in its Rupelian forms (Fig. 5a). Finally, *N. striatus* and *N. vascus* were
501 included among the key species with sigmoidal filaments (see Baudagel-Fadel 2018, p. 461, fig.
502 6.36). It should be noted, that 7-8 subspecies of *N. striatus* were described. Some authors have
503 emphasized that septal traces may be curved at the center (Nemkov, 1967).
504 The following internal features are characteristic for *N striatus*: in the first 1-2 internal whorls,
505 the diameter of the proloculus ranging from 0.22 to 0.3 mm, the radius of 5 whorls being 2.0–2.5

mm, and the radius of 6 whorls being 2.5–3 mm (Schaub, 1981, pl. 53, Figs. 29, 37). The Rupelian representatives of *N. striatus* group from Malishka differ from the Priabonian ones primarily by a slightly looser spiral (the radius of 5whorls is 2.3 - 2.5 mm) and somewhat more curved traces of filaments. Therefore, we refer to this form as *N.* cf. *striatus*. This species also resembles *N. cyrenaicus* of *N. discorbinus* group, but *N. cyrenaicus* is characterized by a larger proloculus and belongs to the Bartonian age. We agree with Nemkov, who placed *N. striatus* in the same group as *N. discorbinus* (Nemkov, 1967). There was some confusion when *N. striatus* was identified as *N. vascus,* and *N. vascus* as *N. striatus* (see Baudagel-Fadel 2018, pl. 6.21, figs 8, 9, 16). *N. vascus* has a smaller test and proloculus and more compressed and regular spiral than *N. striatus* (Schaub, 1981). Besides, *N. vascus* is present in Oligocene deposits from several other sections of Armenia, including Malishka, along with Oligocene reticulate Nummulites (Zakrevskaya et al., 2014). However, *N. cf. striatus* was found together with *N. fichteli* only in Malishka. The small difference from *N. striatus striatus* allow us to assume the presence of a new morphotype of *N. striatus* in the Rupelian.

During the Paleogene, Armenia was situated between the Tethyan and Peritethyan paleogeographic realms. The comparison of bioevents in LBF near the E/O boundary between Armenia and neighboring regions shows that, during this time Armenia was palaeobiogeographically closest to the Mediterranean region. Following to Cahuzac & Poignant (1997) six genera of LBF (*Pellatispira, Orbitolites, Discocyclina, Orbitoclypeus, Asterocyclina, Linderina*) extended in the base of Rupelian. The same genera with the exception of *Linderina*, disappear in Armenia. The common species of *Nummulites* and *Operculina* appeared in lower Rupelian of these regions. The differences between LBF of Armenia and the Central Tethys (Mediterranean, Southeast Asia) are notable, particularly in the absence of porcelaneous and agglutinated foraminifera, as well as the presence of new species of *Heterostegina* and *Spiroclypeus* in Armenia. Interestingly, the change in LBF at the Oligocene boundary in Tanzania (marked by the extinction of genera and the appearance of new taxa within *Nummulites*) (Cotton & Pearson, 2011) shows a similarity to the bioevents in Armenia. In neighboring regions of the Northern Peritethys (Georgia, North Caucasus, Azerbaijan), Oligocene *Nummulites* (such as *N. vascus*) were found only in Georgia. As in Armenia,

porcelaneous and agglutinated LBF are absent in these regions. Therefore, the transitional position of Armenia is clearly reflected in its foraminiferal composition.

The planktonic foraminiferal assemblages are typical of subtropical pelagic environments (Pearson et al., 2006) and some biostratigraphic markers allow for the identification of Eocene-Oligocene boundary zones. The Eocene-Oligocene boundary (EOB) is defined at the Massignano stratotype in Italy and is marked by the extinction of both *Hantkenina* and *Cribrohantkenina* species. The zonal marker, *Hantkenina alabamensis* (HO), which typically marks the E16/O1 boundary (Berggren & Pearson, 2005), was not found. However, the criterion of the extinction of the foraminiferal family Hantkeninidae is not applicable to the Malishka section. Thus alternative biostratigraphic markers for the definition of the boundary in this region is necessary. The highest occurrences (HO) of *Parasubbotina hagni* (within E16 zone), *Subbotina jacksonensis*, *S. linaperta*, *S. yeguaensis*, and *Turborotalia cerroazulensis* were used to mark the top of Zone E16 (Pearson et al., 2006). Consequently, the HO of *T. cerroazulensis* was used to mark the E16/O1 boundary (sample M1609 in Fig. 6). Samples M1602–M1609 were assigned to *Hantkenina alabamensis* Highest Occurrence Zone (HOZ) (Zone E16).

The transition into Zone O1 was identified based on the lowest occurrences (LO) of *Globigerinella obesa* (within O1 zone) (Spezzaferri et al., 2018), *Dentoglobigerina tripartita*, and *D. venezuelana* (Wade et al., 2018). The lowest occurrence of *D. venezuelana* is not well constrained on a global scale. Observations from Deep Sea Drilling Project (DSDP) Site 612 and from Armenia suggest that *D. venezuelana* evolved during the late Eocene, with confirmed occurrences from the lower Oligocene Zone O1 (Leckie et al., 1993). Notably, the LO of *D. venezuelana* was observed in sample M1606 (Fig. 6).

Dentoglobigerina taci first appears in the upper Eocene and persists into the Oligocene (Pearson & Wade, 2015) and *Subbotina tecta*, which has a restricted range from the Zone E16 to O1, provides additional stratigraphic control. The Highest Occurrence (HO) of *Subbotina tecta* (Pearson & Wade, 2015) indicates the top of the O1 zone. The zonal marker, *P. naguewichiensis,* the HO of which marks O1/O2 boundary (Berggren & Pearson, 2005) was not found, so we used the HO of *Turborotalia increbescens* as the marker for the O1/O2 boundary (Pearson et al., 2018). As a marker of the top of the O1 zone, we used the HO of *T. increbescens* (Pirson et al., 2018). For the top of Zone O2, we used the HO of the nominate taxon *Turborotalia*

565 *ampliapertura* (Berggren & Pearson, 2005) as a zonal marker (Wade et al. 2011). The Zone O2
566 is characterized by the LO of *Dentoglobigerina larmeui*, *Globoturborotalita*
567 *pseudopraebulloides* (Spezzaferri et al., 2018; Wade et al., 2018), and *Paragloborotalia*
568 *pseudocontinuosa* (Leckie et al., 2018). The highest occurrence of *Turborotalia ampliapertura* at
569 the top of Zone O2 was used to define the O2/O3 boundary observed in sample M1618 (Fig. 5).
570

571 **6. Conclusion**

572 The 46-meter-thick Malishka section sedimentary succession in Armenia offers an uninterrupted
573 record of deposits spanning from the upper Eocene to the lower Oligocene. This section provides
574 valuable insight into sedimentation during a period characterized by significant climatic events.
575 The shallow-marine carbonate series, consisting of abundant coarse-grained deposits, including
576 conglomerates and volcanic pebble-bearing limestones, indicates a ramp setting. The sediment
577 composition and the sedimentary structures of the beds suggest that these deposits were likely
578 formed near the mean storm wave base. The lower Oligocene greywacke and coarse-grained
579 sandstone, interbedded within a marl succession, are interpreted as having been produced by
580 submarine landslides, massive slumping, or dense, sediment-laden, gravity-driven turbidity
581 flows. The chemical composition of claystones and siltstones, particularly the MgO/CaO ratios,
582 suggests stable weathering conditions with slight fluctuations, further reflecting the transitional
583 climate during this time.
584 This research, by integrating biostratigraphy with lithology, as well as recent systematics of
585 microbiota, has enabled the development of an updated biozonations for LBF and PF in the
586 Malishka section, Armenia. The LBF demonstrate significant abundance and diversity in the
587 upper Eocene sediments, while the Oligocene LBF are represented only by five species of
588 *Nummulites*. The Malishka section, which spans the Eocene-Oligocene transition, corresponds to
589 the PF zones E16, O1, O2, and O3, as well as the LBF zones SBZ20 and SBZ21. The absence of
590 the typical zonal marker, *Hantkenina alabamensis* (HO), prompted the use of alternative markers
591 to define the key boundaries. Specifically, the HO of *Turborotalia cerroazulensis* was used to
592 mark the E16/O1 boundary, while the HOs of *T. increbescens* and *T. ampliapertura* were
593 employed to define the O1/O2 and O2/O3 boundaries, respectively.
594

Acknowledgements

We cordially thank the collaborator of Paleontological Institute RAS E.A. Zhegallo for providing the photographs of planktonic foraminifera. We are grateful to Dr. F. Hayrapetyan (the Institute of Geological Sciences of the Armenian National Academy of Sciences) for organization of field trips in 2013−2014. This work was supported by funding from the Ministry of Education, Science, Culture and Sports (MESCS) of the Republic of Armenia, the Higher Education and Science Committee (Project 18RF-090), and the Russian Foundation for Basic Research (RFBR) under project 18-55-05017.

References

Adams, G. (1988). Septa, septal traces and septal filaments in the foraminiferal genus Nummulites Lamarck: Journal of Micropaleontology, v. 7:89-102.

Aigner, T. (1983). Facies and origin of Nummulitic buildups: an example from the Gisa Pyramids Plateau (Middle Eocene, Egypt). Neues Jahrb. Geol. Paläontol., v. 166(3):347–368.

Avagyan, A., Sosson, M., Sahakyan, L., Sheremet, Y., Vardanyan, S., Martirosyan, M., and Muller, C. (2018). Tectonic evolution of the South-Eastern margin of the Ararat basin, (Lesser Caucasus, Armenia): Journal of Petroleum Geology, v. 41(4):495−511.

Baccelle, L., and Bosellini, A. (1965). Diagrammi per la stima visiva della composizione percentuale nelle rocce sedimentarie. – Annali della Univetrsite di Ferrara, Sezione IX, Science Geologische e Paleontologiche, 1:59-62.

Berggren, W.A., Kent, D.V., Swisher I., C.C., and Aubry, M.-P. (1995). A revised Cenozoic geochronology and chronostratigraphy, *in* Berggren, W. A., Kent, D. V., Aubry, M. -P., and Hardenbol, J. (eds), Geochronology, Time Scales and Global Stratigraphic Correlations: SEPM (Society for Sedimentary Geology) Special Publication No. 54:129−212.

Berggren, W.A., and Pearson, P.N. (2005). A revised tropical to subtropical planktonic foraminiferal zonation of the Eocene and Oligocene: Journal of Foraminiferal Research, v. 35:279–298.

622 Blow, W.H. (1979). The Cainozoic Globigerinida: A Study of the Morphology, Taxonomy,
623 Evolutionary Relationships and the Stratigraphical Distribution of Some Globigerinida (Mainly
624 Globigerinacea). E.J. Brill, Leiden. 3 Vols 1413 p.
625 BouDaghel-Fadel, M.K. (2018). Evolution and geological significance of larger benthic
626 foraminifera. Second Edition, 702p., https://doi.org/10.2307/j.ctvqhsq3
627 Bosence, D.W.J., 1983. Coralline algal reef frameworks. Journal of the Geological
628 Society,140:365-376.
629 Brasier, M., and Donahue, J. (1985). Barbuda – an emerging reef and lagoon complex on the
630 edge of the Lesser Antilles island arc. Journal of the Geological Society, 142:1101-1117.
631 Cahuzac, B. and Poignant, A. (1997). Essai de biozonation de l'Oligo-Miocène dans les bassins
632 européens à l'aide des grands foraminifères néritiques. Bulletin de la Societé géologique de
633 France, v. 168:155−169.
634 Cotton, L. and Pearson, P.N. (2011). Extinction of larger benthic foraminifera at the
635 Eocene/Oligocene boundary: Paleogeography, Paleoclimatology, Paleoecology. V. 33(3-4):281-
636 296. https://doi.org/10.1016/j.palaeo.2011.09.008
637 Cotton, L., Zakrevskaya, E., Boon, A., Asatryan, G., Hayrapetyan, F., Israyelyan, A., Krijgsman,
638 W., Papazzoni, G., Pearson, P., Razumovskiy, A., Renema, W., Shcherbinina, E., Wade, B.
639 (2017). Integrated stratigraphy of the Priabonian (upper Eocene) Urtsadzor section, Armenia:
640 Newsletters on Stratigraphy, v. 50(3):269 295.
641 Coxall, H.K. and Pearson, P.N. (2007). The Eocene–Oligocene transition: *in* Williams, M.,
642 Hayward, A., Gregory, J., Schmidt, D. (eds), Deep Time Perspectives on Climate Change:
643 Marrying the Signal from Computer Models and Biological Proxies: Special Publication 2.
644 London, UK: Te Micropalaeontological Society (the Geological Society):351−387.
645 Dunham, R.J. (1962). Classification of carbonate rocks according to depositional texture, in
646 Ham, W.E., ed., Classification of Carbonate Rocks: American Association of Petroleum
647 Geologists Memoir:108–121.
648 Embry, A.P., Klovan, J.E. (1971). A Late Devonian reef tract on northeastern Banks Island,
649 Northwest Territories // Bull. Can. Petrol. Geol. v. 19:730–781.
650 Evans, D., Sagoo, N., Renema, W., Cotton, L. J., Müller, W., Todd, J. A., Saraswati, P. K.,
651 Stassen, P., Ziegler, M., Pearson, P. N., Valdes, P. J. and Affek, H. P. (2018). Eocene greenhouse

climate revealed by coupled clumped isotope-Mg/Ca thermometry, Proc. Natl. Acad. Sci., 115(6):1174 – 1179, doi:10.1073/pnas.1714744115

Flügel, E. (2004). Microfacies of Carbonate Rocks, Analysis, Interpretation and Application. Berlin: Springer-Verlag, 633 p.

Gabrielian, A., 1964. Paleogene and Neogene of Armenian SSR:. Akademiya Nauk Armyanskoi SSR, Yerevan, 299 p. (In Russian)

Galoyan G. (2008). Etudes petrologiques, geochimiques et geochronologiques des ophiolites du Petit Caucase (Armenie). These de Docteur en Sciences de l'Universite de Nice-Sophia Antipolis. 287p.

Grigorian, S.M. (1986). *Nummulites and Orbitoides* of Armenian SSR: Akademiya Nauk Armyanskoi SSR, Yerevan. 216 p. (In Russian).

Grigorian, S.M. (1979). Nummulitids of the upper Eocene and Oligocene deposits of south-western part of Armenian SSR: Akademiya Nauk Armyanskoi SSR, Yerevan. 100 p. (In Russian).

Grigoryan, T. E., and Sahakyan, K. (2019). Cleaning method for planktonic foraminifera shells: An optimised procedure: National Akademii of Sciences RA, Earth Sciences, v. 72 (2):84−85.

Hadi, M., Mosaddegh, H., Abbassi, N. (2016). Microfacies and biofabric of nummulite accumulations (bank) from the Eocene deposits of Western Alborz (NW Iran). Journal of African Earth Sciences, v. 124:216–233

Hayrapetyan, F.A. (2001). Subdivision of middle-upper Eocene (Zovashen formation) of Azat River valley by small foraminifera. Izv. of National Akademii of Sciences RA, Earth Sciences, Yerevan, v. 2:3−5 (In Russian).

Hayrapetyan, F.A. (2009). Zonal subdivision of Paleogene deposits of Vedi River valley by small foraminifera (Arax tectonic zone): Izv. of National Akademii of Sciences RA, Earth Sciences, Yerevan, v. 2:6−16 (In Russian).

Herb, R., and Hekel, H. (1975). Nummuliten aus dem Obereocaen von Possagno. Schweizerische Paläontologische Abhandlungen 97:113–135 (in German with English abstract).

Houben, A.J.P., van Mourik, C.A., Montanari, A., Coccioni, R., and Brinkhuis, H. (2012). The Eocene-Oligocene transition: Changes in sea level, temperature or both?: Palaeogeography, Palaeoclimatology, Palaeoecology, v. 335–336:75–83.

682 Hutchinson, D. K., Coxall, H. K., Lunt, D. J., Steinthorsdottir, M., Boer A. M. (2021). The
683 Eocene–Oligocene transition: a review of marine and terrestrial proxy data, models and model–
684 data comparisons, *in* Climate of the Past, 17:269-315. https://doi.org/10.5194/cp-17-269-2021
685 Krasheninnikov, V. A., Muzylöv, N. G., and Ptukhian, A. E., 1985. Stratigraphic subdivision of
686 Paleogene deposits of Armenia by planktonic foraminifers, nannoplankton and Nummulites. (Pt
687 I. Reference Paleogene sections of Armenia): Voprosy micropaleontologii, v. 27:130–169.
688 Krasheninnikov, V.A., and Ptukhian, A.E. (1986). Stratigraphic subdivision of Paleogene
689 deposits of Armenia by planktonic microfossils and nummulites. (Regional stratigraphy, zonal
690 scales by planktonic and benthonic microfossils, their correlation): Voprosy micropaleontologii,
691 Moscow, v. 28:60−98 (In Russian with English abstract).
692 Krasheninnikov, V. A., Grigoryan S.M., Martirosian Yu.A, Ptuchian A.E., and Zaporozhets, N.I.
693 (1986). Section Landzhar (USSR, South Armenia), *in* Pomerol, Ch., and Premoli-Silva, I. (eds.),
694 Terminal Eocene Events:). Elsevier Science Publishers, 413p.
695 Krasheninnikov, V.A., and Akhmetiev, M.A. (eds.). (1998). Late Eocene–Early Oligocene.
696 Geological and biotical events: Part 2. Moscow, GEOS, 250 p. (in Russian, English summary).
697 Leckie, R. M., Farnham, C. & Schmidt, M. G. (1993). Oligocene planktonic foraminifer
698 biostratigraphy of Hole 803D (Ontong Java Plateau) and Hole 628A (Little Bahama Bank), and
699 comparison with the southern high latitudes. *Proceedings of the Ocean Drilling Program,*
700 *Scientific Results.* 130: 113-136.
701 Lowenstein, T.K., Hönisch, B. (2017). The Use of Mg/Ca as a Seawater Temperature Proxy. The
702 Paleontological Society Papers, Volume 18: Reconstructing Earth's Deep-Time Climate: 85-100.
703 Lear, C. H., Elderfield, H., and Wilson, P.A. (2000). Cenozoic deep-sea temperatures and global
704 ice volumes from Mg/Ca in benthic foraminiferal calcite: Science, v. 287:269– 272.
705 Lear, C.H., Bailey, R.T., Pearson, P.N., Coxall, H.K., Rosenthal, Y. (2008). Cooling and ice
706 growth across the Eocene-Oligocene transition. Geology 36 (3):251–254.
707 https://doi.org/10.1130/G24584A.1
708 Less, G. (1998). Zonation of the Mediterranean upper Paleocene and Eocene by
709 Orthophragminae: Opera Dela Slovenska Akademija Znanosti in Umetnosti (4), v. 34:21−43.
710 Less, G., and Özcan, E. (2008). The late Eocene evolution of nummulitid foraminifer
711 *Spiroclypeus* in the Western Tethys: Acta Palaeontologica Polonica, v. 53:303–316.

712 Less, G., and Özcan, E. (2012). Bartonian-Priabonian larger benthic foraminiferal events in the
713 Western Tethys: Austrian Journal of Earth Sciences, v. 105(1):129–140.
714 Less, G., Özcan, E., Papazzoni, C.A., and Stockar, R. (2008). The middle to late Eocene
715 evolution of nummulitid foraminifer *Heterostegina* in the Western Tethys: Acta Palaeontologica
716 Polonica, v. 53 (2):317–350.
717 Mateu-Vicens, G., Pomar, L., Ferrandez-Canadel, C. (2012). Nummulitic banks in the upper
718 Lutetian 'Buil level', Ainsa Basin, South Central Pyrenean Zone: The impact of internal waves.
719 Sedimentology. V. 59:527–552.
720 Nikogosian, I. K., Bracco Gartner, A. J. J., Mason, P. R. D., van Hinsbergen, D. J. J., Kuiper, K.,
721 Kirscher, U., Matveev, S., Grigoryan, A., Grigoryan, E., Israyelyan, A., van Bergen, M. J.,
722 Koornneef, J. M., Wijbrans, J. R., Davies, G. R., & Meliksetian, K. (2023). The South Armenian
723 Block: Gondwanan origin and Tethyan evolution in space and time. *Gondwana Research*,
724 S1342937X23001065. https://doi.org/10.1016/j.gr.2023.03.023
725 Nemkov, G.I. (1967). Nummulitides of the Soviet Union and their biostratigraphic significance.
726 Nauka, Moscow (in Russian with English abstract).
727 Özcan, E., Less, G., Okay, A.I., Báldi-Beke, M., Kollányi, K., and Yilmaz, O.I. (2010).
728 Stratigraphy and larger foraminifera of the Eocene shallow-marine and olistostromal units of the
729 southern part of the Thrace Basin, NW Turkey: Turkish Journal of Earth Sciences, v. 19:27–77.
730 doi:10.3906/yer-0902-11
731 Pearson, P.N., Olsson, R.K., Huber, B.T., Hemleben, C., and Berggren, W.A. (2006). Atlas of
732 Eocene Planktonic Foraminifera. Cushman Foundation Special Publication. Allen Press,
733 Lawrence, Kansas, 513 p., 136 pls.
734 Pearson, P.N., and Wade, B.S. (2015). Systematic taxonomy of exceptionally well-preserved
735 planktonic foraminifera from the Eocene/Oligocene boundary of Tanzania: Cushman Foundation
736 Special Publication No. 45:1−85.
737 Pearson, P. N., Olsson, R. K., Spezzaferri, S., and Leckie, R. M. (2018). Taxonomy,
738 biostratigraphy, and phylogeny of Oligocene Globanomalinidae (Turborotalia and
739 Pseudohastigerina), *in* Wade, B. S., Olsson, R. K., Pearson, P. N., Huber, B. T., and Berggren,
740 W. A. (eds), Atlas of Oligocene Planktonic Foraminifera: Cushman Foundation for Foraminiferal
741 Research, Special Publication 46, (Chap 14):403−414.

Reading, H.G., Collinson, G.D., Allen, F.A. et al. (1996). Sedimentary Environments: Processes, Facies and Stratigraphy / 3rd edition. Oxford: Blackwell Science Ltd. 688 p.

Rezeau, H., Moritz, R., Leuthold, J., Hovakimyan, S., Tayan, R., and Chiaradia, M. (2017). 30 Myr of Cenozoic magmatism along the Tethyan margin during Arabia-Eurasia accretionary orogenesis (MeghrieOrdubad pluton, southernmost Lesser Caucasus): Lithos,v. 288:108−124.

Sahakyan, L., Bosch, D., Sosson, M., Avagyan, A., Galoyan, Gh., Rolland, Y., Bruguier, O., Stepanyan, Zh., Galland, B., and Vardanyan, S. (2017a). Geochemistry of the Eocene magmatic rocks from the Lesser Caucasus area (Armenia): evidence of a subduction geodynamic environment: Tectonic Evolution of the Eastern Black Sea and Caucasus, Geol. Soc. of London, Special Volume 428:73−98.

Sahakyan, L.H., Avagyan, A.V., Sosson, M., Zakrevskaya, E.Yu., and Grigoryan, T.E., 2017b Tectonic conditions and evolution of Paleogene sedimentation of Shagap syncline: Proceedings of the NAS RA: Earth Sciences, v. 70 (1):24−35.

Sahakyan, L. Grigoryan, T., Avagyan, A., Zakrevskaya, E., Stepanyan, Zh., and Hayrapetyan, A. (2020). Upper Eocene-Lower Oligocene Shaghap reef (Armenia): Composition and paleoenvironment: Proceedings of the NAS RA: Earth Sciences, v. 73 (1):3−15.

Sahakyan-Gezalyan, N.A, Martirosyan, Yu.A, and Bubikyan, C.A. (1967). Biostratigraphicheskoe raschlenenie tretichnykh otlozhenii yugo-zapadnoi chasti Armyanskoi SSR: Izvestiya Akademii Nauk Armyanskoi SSR, Earth Sciences, Yerevan, v. 20 (3):85−92 (in Russian).

Sargsyan, H. (1989). Regional Geotectonics of Armenian SSR: Proceedings of Yerevan State University, Yerevan, 276 p.

Sarkisova, E., Amon, E., Zakrevskaya, E., and Sahakyan, L. (2020). New data on Middle Eocene (Paleogene) radiolarians of Southern Armenia: The Landzhar Reference Section: Bulletin of the Moscow Society of Naturalists, Geological Department t.95, n.1:14−41.

Schaub, H. (1981). *Nummulites* et Assilines de la Tethys Paléogène. Taxonomie, 20 phylogénèse et biostratigraphie : Schweizerische Paläontologische Abhandlungen 104– 21, 106, Bâle: 1–236 + 2 Atlas (in French).

770 Serra-Kiel, J., Hottinger, L., Caus, E., Drobne, K., Ferrandez, C. et al. (1998). Larger
771 foraminiferal biostratigraphy of the Tethyan Paleocene and Eocene: Bulletin de la Societé
772 géologique de France, v. 169 :281−299.
773 Shcherbinina, E., Yakovleva, A., and Zakrevskaya, E. (2017). Eocene–Early Oligocene
774 nannofossils and palynomorphs from the Landzhar Section, Southern Armenia: Zonal
775 stratigraphy and paleoecology: Stratigraphy and Geological Correlation, v. 25 (5):557–580. doi:
776 10.1134/S0869593817050069
777 Sosson, M., Rolland, Y., Muller, C., Danelian, T., Melkonyan, R., Kekelia, S., Adamia, S.,
778 Babazadeh, V., Kangarli, T., Avagyan, A., Galoyan, G., and Mosar, J. (2010). Subductions,
779 obduction and collision in the Lesser Caucasus (Armenia, Azerbaijan, Georgia), new insights, *in*
780 Sosson, S., Kaymakci, N., Stephenson, R., Bergerat, F., and Starostenko, V. (eds.), Sedimentary
781 Basin Tectonics from the Black Sea and Caucasus to the Arabian Platform: Geological Society
782 of London, Special Volume 340:329–352.
783 Spezzaferri, S., Olsson, R. K., Hemleben, C., Wade, B. S., Coxall, H. K. (2018). Taxonomy,
784 biostratigraphy, and phylogeny of Oligocene *Globigerina*, *Globigerinella*, and *Quiltyella* n. gen.
785 In: Pearson, P. N., Olsson, R. K., Hemleben, C., Wade, B. S., Berggren, W. A., Coxall, H. K.
786 (Eds.), *Taxonomy, Biostratigraphy, and Phylogeny of Oligocene and Lower Miocene Planktonic*
787 *Foraminifera*. Cushman Foundation Special Publication No. 46, pp. 179–214.
788 Vanden Berghe, N., Hilgen, F.J., Speijer, R.P., Ogg, J.G., Gradstein, F.M., Hammer, O., Hollis,
789 C.J., and Hooker, J.J. (2012). The Paleogene Period, *in* Gradstein, R. M., et al. (eds.). The
790 Geologic Time Scale 2012. Amsterdam: Elsevier:855–923.
791 Wade, B. S., Pearson, P. N., Berggren, W. A., and Pälike, H. (2011). Review and revision of
792 Cenozoic tropical planktonic foraminiferal biostratigraphy and calibration to the geomagnetic
793 polarity and astronomical time scale: Earth-Science Reviews, v. 104:111–142.
794 Wade, B. S., Olsson, R. K., Pearson, P. N., Huber, B. T., and Berggren, W. A., eds. (2018). Atlas
795 of Oligocene Planktonic Foraminifera. London: Cushman Foundation for Foraminiferal
796 Research, 524 p.
797 Zakrevskaya, E., Shcherbinina, K., and Hayrapetyan, F. (2014). The Bartonian and Priabonian
798 boundaries in southern Armenia: problems and solutions: Field trip guide book. VNII
799 Geosystem, Moscow, 49 p.

800 Zakrevskaya, E.Yu., Bugrova, E.M., Shcherbinina, E.A., Sahakyan L.G., Hayrapetyan, F.A.,
801 Grigoryan, T.E., and Woloshina, O.V. (2017). Micropaleontological characteristics of middle
802 Eocene – lower Oligocene of Landzhar and Urtsalandzh sections, Southern Armenia: Bulletin of
803 Moscow Society of Naturalists, Geological Series, v. 92, part 5:60–85.
804 Zakrevskaya, E., Less G., Bugrova, E., Shcherbinina, E., Grigoryan, T., and Sahakyan, L.
805 (2020). Integrated biostratigraphy and benthic foraminifera of the middle-upper Eocene 1
806 deposits of Urtsadzor section (Southern Armenia): Turkish Journal of Earth Sciences, v.
807 29:896−945. DOI: 10.3906/yer-1912-6.
808 Zaporozhets, N.I. (1989). Palinoassemblages and phytoplankton from upper Eocene-Oligocene
809 deposits of Borehole 1 (Landzhar, Armenia): Paleofloristica and Stratigraphy of Phanerozoic.
810 GIN AS USSR, Moscow:85−103 (In Russian).
811

Declaration of Interest Statement

The authors of the manuscript titled "*Diversity and Biolithostratigraphy of Foraminifera from the Upper Eocene–Lower Oligocene Malishka Section, Armenia*" declare that this manuscript is original, has not been published previously, and is not currently under consideration for publication elsewhere.

The authors confirm that the manuscript has been read and approved by all listed authors and that there are no other individuals who meet the criteria for authorship but are not included. The order of authors has been agreed upon by all contributors.

The authors acknowledge that the Corresponding Author, Lilit Sahakyan, is the primary contact for the editorial process. She is responsible for coordinating communication with the journal, handling submissions and revisions, and providing final approval of proofs.

Authors' Contributions Statement

Grigoryan Taron: Methodology, Formal analyses, Writing – Original Draft

Lilit Sahakyan: Supervision, Conceptualization, Data curation, Writing – Original Draft, Review & editing

Elena Zakrevskaya: Data curation, Formal analyses, Writing – Original Draft

Pavel Fokin: Formal analyses, Methodology, Writing – Original Draft

Ara Avagyan: Methodology.

Data Availability Statement

The datasets generated and analyzed during the current study are available from the corresponding author upon request.



L. Sahakyan for all authors

03.03.2025